Available online at www.sciencedirect.com
SCIENCE DIRECT®
Neural Networks xx (2005) 1–31
Neural Networks
www.elsevier.com/locate/neunet

A robot model of the basal ganglia: Behavior and intrinsic processing☆

Tony J. Prescott[a,*], Fernando M. Montes González[b], Kevin Gurney[a], Mark D. Humphries[a], Peter Redgrave[a]

[a]*Adaptive Behavior Research Group, Department of Psychology, University of Sheffield, Sheffield, Western Bank, South Yorkshire, Sheffield S10 2TN, UK*
[b]*Department de Fisica e Inteligencia Artificial, Universidad Veracruzana, Xalapa, Veracruz, Mexico*

Received 13 August 2004; accepted 9 June 2005

Abstract

The existence of multiple parallel loops connecting sensorimotor systems to the basal ganglia has given rise to proposals that these nuclei serve as a selection mechanism resolving competitions between the alternative actions available in a given context. A strong test of this hypothesis is to require a computational model of the basal ganglia to generate integrated selection sequences in an autonomous agent, we therefore describe a robot architecture into which such a model is embedded, and require it to control action selection in a robotic task inspired by animal observations. Our results demonstrate effective action selection by the embedded model under a wide range of sensory and motivational conditions. When confronted with multiple, high salience alternatives, the robot also exhibits forms of behavioral disintegration that show similarities to animal behavior in conflict situations. The model is shown to cast light on recent neurobiological findings concerning behavioral switching and sequencing.

Keywords: Basal ganglia; Action selection; Behavior switching; Embodied computational neuroscience; Robot; Rat

1. Introduction

The basal ganglia are a group of highly interconnected central brain structures with a critical influence over movement and cognition. Interest in these structures derives in part from their importance for a cluster of brain disorders that includes Parkinson's disease, Huntington's disease, Tourette's syndrome, schizophrenia, and attention deficit hyperactivity disorder, and has driven more than a century of neurobiological study. This extensive research effort has given rise to a wealth of relevant data, and consequently a pressing need for a better functional understanding of these structures. The basal ganglia, therefore, present one of the most exciting prospects for computational modeling of brain function and have been the focus of extensive modeling research efforts (for reviews see Gillies & Arbuthnott, 2000; Gurney, Prescott, Wickens, & Redgrave, 2004; Houk, Davis, & Beiser, 1995; Prescott, Gurney, & Redgrave, 2002; Wickens, 1997).

A recurring theme in the basal ganglia literature is that these structures operate to release inhibition from desired actions while maintaining or increasing inhibition on undesired actions (Cools, 1980; Denny-Brown & Yanagisawa, 1976; Hikosaka, 1994; Mink, 1996; Robbins & Brown, 1990; Wickens, 1997). In our own theoretical work (Prescott, Redgrave, & Gurney, 1999; Redgrave, Prescott, & Gurney, 1999a) we have developed the idea that the basal ganglia acts as an *action selection* mechanism—resolving conflicts between functional units that are physically separated within the brain but are in competition for behavioral expression. We have shown how this proposal relates to known anatomy and physiology and meets several high-level computational requirements for an effective action selection device. In line with this hypothesis we also embarked on a program of modeling the circuitry of the basal ganglia and related structures at several levels of abstraction. A key focus has been to investigate 'system' level models of the basal ganglia constrained by the known functional anatomy in which neural populations are represented by simple leaky integrator units (Gurney, Prescott, & Redgrave, 2001a,b; Gurney, Humphries,

☆UK Engineering and Physical Sciences Research Council (EPSRC) GR/R95722/01.
* Corresponding author. Tel.: +44 114 2226547, fax: +44 114 2766515.
E-mail address: t.j.prescott@sheffield.ac.uk (T.J. Prescott).

0893-6080/$ - see front matter © 2005 Published by Elsevier Ltd.
doi:10.1016/j.neunet.2005.06.049

Wood, Prescott, & Redgrave, 2004; Humphries & Gurney, 2002). At lower levels of neurobiological detail we have studied the patterning of signals encoded by trains of action potentials ('spikes') (Humphries, 2002; Humphries & Gurney, 2001), and have investigated biophysical models of the membrane dynamics of striatal neurons (Wood, Gurney, & Wilson, 2004). Studies at all of these levels have generated complementary results confirming that the biological architecture of the basal ganglia can operate as an effective selection mechanism. In our view, however, this *computational neuroscience* approach, in which specific brain systems are modeled in isolation of the wider context, still leaves many important questions unanswered. First, we are left wondering how best to interpret the inputs and outputs of the model—we might choose to think of inputs as, say, 'sensory' signals, or of outputs as 'motor' signals, but such assignments are essentially ungrounded. Second, without locating a model within any wider context, we are unable to judge whether it can fulfill its hypothesized functional role within a more fully specified control architecture. Third, without any linkage to sensory and motor systems, we may question whether a model could cope with noisy or ambiguous sense data, or as part of a system challenged with coordinating the movements of real effector systems. Finally, without the context of multiple demands, such as the need to maintain physical integrity, avoid threats, and discover and exploit resources, we will be unsure whether or not a model can meet some of the basic requirements for adaptive behavior. In this article we, therefore, describe an embedding of the system-level model of the basal ganglia and associated thalamocortical connections within the control architecture of a small mobile robot engaged in a simulated foraging task that requires the robot to select appropriate actions under changing sensory and motivational conditions and thereby generate sequences of integrated behavior. We describe the methodology we are applying as *embodied computational neuroscience*. Preliminary results for the robot model have been described in (Montes Gonzalez, Prescott, Gurney, Humphries, & Redgrave, 2000), and a version of the model has been shown to have better selection properties than a standard *winner-takes-all* selection mechanism in a robotic survival task (Girard, Cuzin, Guillot, Gurney, & Prescott, 2003). The current article, however, provides the first full account of the robot embedding of the basal ganglia model together with an extensive evaluation of the model's behavior in comparison to relevant neurobehavioral studies. We also present results showing the behavior of the robot model when faced with multiple high-salience alternatives, and draw comparisons with studies of animal behavior in conflict situations.

The remainder of the article is organized as follows. The action selection hypothesis of the basal ganglia and related modeling work is reviewed in Section 2. The motivation for the robot basal ganglia model, full details of the robot implementation, and a summary of action selection metrics, are described in Section 3 (and the accompanying appendices). Section 4 then describes the results of three experiments: experiment 1, a systematic search of a salience space using a disembodied version of the extended basal ganglia model (extending earlier analyses of this model by Humphries and Gurney, 2002); experiment 2, our main investigation of the action selection by the robot basal ganglia model; and experiment 3, an investigation of robot behavior in the context of high salience alternatives. Section 5 provides our discussion of the experimental results focusing on comparisons with biological data.

2. Background: the basal ganglia viewed as an action selection device

There have been many excellent summaries of the functional anatomy of the basal ganglia (e.g. Gerfen & Wilson, 1996; Mink, 1996; Smith, Bevan, Shink, & Bolam, 1998), the following, therefore, focuses on those aspects most relevant to understanding the models discussed below.

The principle structures of the rodent basal ganglia (Fig. 1a) are the striatum (consisting of the caudate, the putamen, and the ventral striatum), the subthalamic nucleus (STN), the globus pallidus (GP), the substantia nigra (SN, consisting of the *pars reticulata* SNr and *pars compacta* SNc), and the entopeduncular nucleus (EP) (homologous to the globus pallidus internal segment, or GPi, in primates). These structures are massively interconnected and form a functional sub-system within the wider brain architecture (Fig. 1b).

The input nuclei of the basal ganglia are the striatum and the STN. Afferent connections to both of these structures originate from virtually the entire brain including cerebral cortex, many parts of the brainstem (via the thalamus), and the limbic system. These connections provide phasic excitatory input. The main output nuclei are the substantia nigra pars reticulata (SNr), and the entopeduncular nucleus (EP). These structures provide extensively branched efferents to the thalamus (which in turn project back to the cerebral cortex), and to pre-motor areas of the midbrain and brainstem. Most output projections are tonically active and inhibitory.

To understand the intrinsic connectivity of the basal ganglia it is important to recognize that the main projection neurons from the striatum (medium spiny cells) form two widely distributed populations differentiated by their efferent connectivity and neurochemistry. One population contains the neuropeptides substance P and dynorphin, preferentially expresses the D1 subtype of dopamine receptors, and projects primarily to the output nuclei (SNr and EP). In the prevailing informal model of the basal ganglia (Albin, Young, & Penney, 1989) this 'D1 striatal' projection constitutes the so-called direct pathway to the output nuclei. Efferent activity from these neurons suppresses the tonic inhibitory firing in the output structures

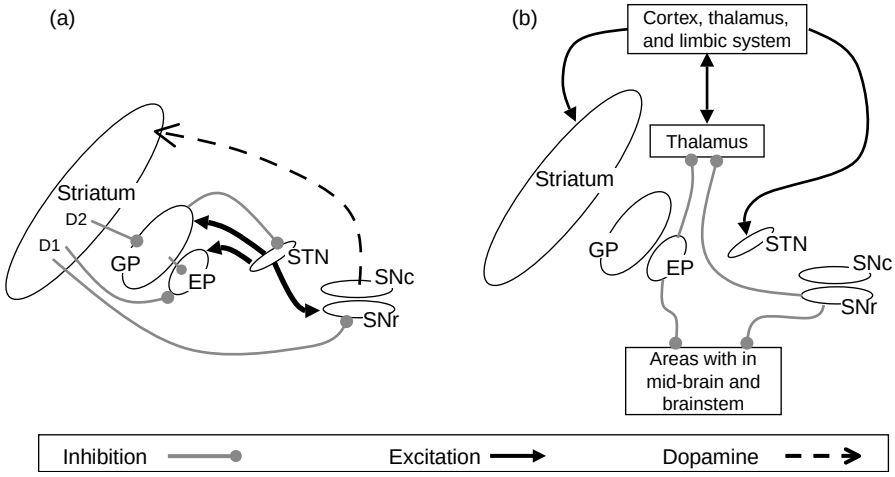

Fig. 1. Basal ganglia anatomy of the rat: (a) internal pathways, (b) external pathways. Not all connections are shown. Abbreviations: STN, subthalamic nucleus; EP, entopeduncular nucleus; GP, globus pallidus; SNc, substantia nigra pars compacta; SNr, substantia nigra pars reticulata; D1; D2, striatal neurons preferentially expressing dopamine receptors subtypes D1 and D2.

which in turn disinhibits targets in the thalamus and brainstem. A second population of striatal projection neurons contains enkephalin and preferentially expresses D2 subtype dopamine receptors. This group projects primarily to the globus pallidus (GP) whose tonic inhibitory outputs are directed both to the output nuclei (SNr and EP) and to the STN. The inhibitory projection from these 'D2 striatal' neurons constitutes the first leg of an indirect pathway to the output nuclei. Since this pathway has two inhibitory links (Striatum-GP, GP-STN), followed by an excitatory one (STN-EP/SNr), its net effect is to activate output nuclei thereby increasing inhibitory control of the thalamus and brainstem.

The main source of dopamine innervation to the striatum is the substantia nigra pars compacta (SNc). Dopaminergic modulation of basal ganglia is generally considered to act at two time-scales (Grace, 1991; Walters, Ruskin, Allers, & Bergstrom, 2000). One is a short-latency phasic response (100 ms burst) that correlates with the onset of biologically significant stimuli and appears to be critical for some forms of incentive learning (Redgrave, Prescott, & Gurney, 1999b; Schultz, Dayan, & Montague, 1997), the other is a tonic level of activity (1–8 Hz) that is altered by various brain pathologies, such as Parkinson's disease, and in the normal brain may be subject to modulation by structures such as the frontal cortex. Interestingly, the D1 and D2 striatal populations respond differently to variations in dopaminergic transmission. Whilst a range of effects have been reported, one simplifying hypothesis, that accounts for a significant proportion of available findings, is that dopamine enhances the effectiveness of other synaptic inputs when acting via D1 receptors (Akkal, Burbaud, Audin, & Bioulac, 1996) whilst reducing such efficacy when acting at D2 receptors (Gerfen, Engber, Mahan, Susel, Chase and Monsma, 1990; Harsing & Zigmond, 1997). This arrangement seems to provide dopaminergic control of a 'push/pull' mechanism subserved by the direct (inhibitory) and indirect (net excitatory) basal ganglia pathways. The effects of variations in this tonic dopamine level on our robot model are the subject of a separate article; in the current work we report results in which the simulated dopamine level is fixed at an intermediate level. Likewise, the current article does not address the problem of learning (and the role of dopamine therein), but the logically distinct question of whether the basal ganglia are suitably configured to support action selection in an embodied agent.

A key assumption of our basal ganglia model is that the brain is processing, in parallel, a large number of sensory and cognitive streams or *channels*, each one potentially carrying a request for action to be taken. For effective behavior, the majority of these requests must be suppressed to allow the expression of only a limited number (perhaps just one). This channel-based scheme is consistent with evidence that basal ganglia input occurs via a series of topographically organized, parallel processing streams (Alexander & Crutcher, 1990). The action selection hypothesis of the basal ganglia further suggests that the activity of cell populations in the striatum and STN encodes the *salience*, or propensity for selection, of candidate actions. At the same time, the basal ganglia output structures, SNr and EP, are viewed as *gating* candidate actions via a reduction in their inhibitory output for winning channels. When considered in isolation of the wider brain architecture, this action selection thesis is best restated in terms of the context-neutral problem of 'signal selection'; in other words, the proposal is that large signal inputs at striatum and STN select for low signal outputs at EP/SNr.

From a signal selection perspective multiple mechanisms within the basal ganglia and related circuitry appear to be suitably configured to resolve conflicts between competing channels and provide the required clean and rapid switching between winners. Our initial system-level model of

the basal ganglia (Gurney et al., 2001a,b) focused on the following candidate selection mechanisms.

First, at the cellular level considerable interest has focused on an intrinsic property of striatal projection neurons such that, at any given moment, a majority of cells are in an inactive 'down-state', and can only be triggered into an active 'up-state' (where they can fire action potentials) by a significant amount of coincident input (Wilson & Kawaguchi, 1996). This bistable behavior could act as a high-pass filter to exclude weakly supported 'requests'.

Second, computational theory suggests that a *feed-forward*, *off-centre*, *on-surround network* is an appropriate mechanism for enhancing signal selection. In the basal ganglia, this type of selection circuit appears to be implemented by a combination of focused striatal inhibition of the output nuclei (the off-centre) and diffuse STN excitation of the same (the on-surround) (Parent & Hazrati, 1995). On closer examination, however, it appears that there are actually two such feed-forward networks in the basal ganglia intrinsic circuitry (see Fig. 2a and b), differentiated by the projection targets of the D1-type and D2-type sub-populations of striatal neurons. One instantiation (Fig. 2a) makes use of EP/SNr as its 'output layer'; since this is clearly consistent with our signal selection hypothesis for the basal ganglia we have designated this circuit the *selection pathway*. However, there is also a second implementation of the feed-forward architecture whose target is the GP (Fig. 2b). Since the efferent connections of the GP are confined to other basal ganglia nuclei it is not immediately clear in what sense this second implementation can contribute to the overall selection task. This question can be resolved by supposing that this second sub-system forms a *control pathway* that functions to regulate the properties of the main selection mechanism. The control signals emanating from GP are evident when the two sub-systems are combined to give the overall functional architecture shown in Fig. 2c.

In our original system-level model, we operationalized the above circuit (Fig. 2c) as a multi-channel system where, for every basal ganglia nucleus, the neural population encoding each channel is simulated by a suitably configured leaky integrator unit. Analytical and simulation studies (Gurney et al., 2001a,b) conducted with this model demonstrated that it has the capacity to support effective switching between multiple competitors. In simulation, two or more channels of the model were provided with afferent input in the form of hand-crafted signals of different amplitude. Results showed that the largest signal input always generates the smallest signal output (thus showing signal selection), and that the system rapidly switches from a currently selected channel to a competing channel that suddenly has a larger input. We were also able to generate signal characteristics in the component circuits of our basal ganglia model that follow similar temporal patterns to single-unit recordings of neural firing in GP (Ryan & Clark, 1991) and SNr (Schultz, 1986).

Humphries and Gurney extended the original model of intrinsic basal ganglia processing to include basal ganglia-thalamocortical loops (Humphries & Gurney, 2002). This work led to the proposal that the thalamic complex—the ventro-lateral (VL) thalamus and thalamic-reticular nucleus (TRN)—acts to provide additional selection-related functionality. Specifically, as shown in Fig. 3, these circuits can be understood as sub-serving two important roles. First, disinhibition of VL thalamic targets by EP/SNr enables a *positive feedback loop* whereby winning basal ganglia channels can increase the activation of their own cortical inputs. Second, the within- and between- channel connections between the TRN and the VL thalamus appear to implement a distal lateral-inhibition network that serves to increase the activity of the most strongly innervated channel at the expense of its neighbors. In simulation, again with hand-crafted signals, the additional selective functions of these extra-basal ganglia mechanisms were found to promote several desirable selection features including cleaner switching between channels of closely matched salience, and the ability to ignore transient salience interrupts. Recently, we have also shown that the model can accommodate new data on striato pallidal projections,

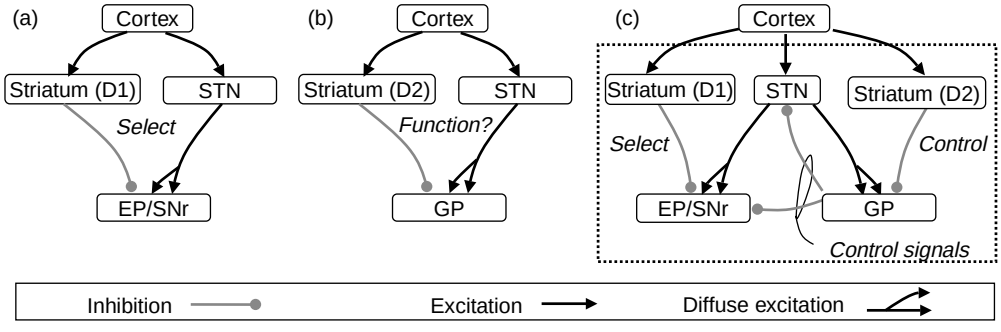

Fig. 2. The basal ganglia viewed as an action selection mechanism. Abbreviations as per Fig. 1. Our analysis of the basal ganglia intrinsic connectivity (Gurney et al., 2001a,b) indicated the presence of two off-centre, on-surround, feed-forward networks. One instantiation: (a) makes use of EP/SNr as its 'output layer' and is designated the *selection* pathway, the second (b) targets GP and is designated the *control* pathway. The control signals emanating from GP are evident when the two sub-systems are combined to give the overall functional architecture shown in Figure c.

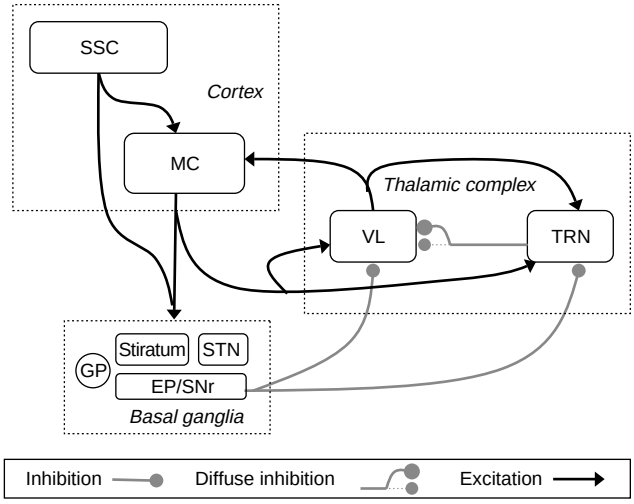

Fig. 3. The extended basal ganglia model of Humphries and Gurney (2002). Abbreviations: SSC, somatosensory cortex; MC, motor cortex; VL, ventro-lateral thalamus; TRN, thalamic-reticular nucleus, others as per Fig. 1. Connectivity within the basal ganglia component of the model is as shown in Fig. 2c. Basal ganglia-thalamocortical loops can be understood as providing additional mechanisms that can contribute to effective action selection. First, the removal of basal ganglia inhibition from VL completes a positive feedback loop to the motor cortex. Second, the diffuse inhibitory connections from TRN to VL, which are stronger between channels than within channels (as indicated by the plain and dotted inhibitory connections in the figure), together with within-channel excitation from VL to TRN, produces a form of mutual inhibition between channels. See text and Humphries and Gurney (2002) for further explanation.

and on local inhibitory connections within the globus pallidus and substantia nigra (Gurney, Humphries et al., 2004; Humphries, Prescott, & Gurney, 2003). Both extensions also appear to enhance the selectivity of the system and, in adding further biological realism, lend further support to the selection hypothesis of basal ganglia function.

An effective action selection mechanism should be sensitive to changes in salience weightings that alter the relative urgency of competing behaviors in a given context. It is less evident, however, how a selection mechanism should respond to changes in salience weightings that leave relative salience unchanged whilst scaling the overall level of the selection competition. The assumption encapsulated by the widely used *winner-takes-all* selection mechanism, for example, is that the overall level of salience is irrelevant (the competitor with highest salience is always preferred). We have previously demonstrated that the selection properties of both the intrinsic (Gurney et al., 2001b) and extended (Humphries and Gurney, 2002) basal ganglia models do not conform to this assumption, but instead, vary according to the overall 'intensity' of the selection competition. We will extend this work below by showing that that the degree of hysteresis, or persistence, of the winning sub-system may change as a consequence of changes in the overall level of salience. Our previous studies noted interesting patterns of 'multiple channel' selection when the model is presented with multiple, high salience alternatives. We, therefore, investigate the behavior of the robot model in these circumstances, and consider possible parallels with observations derived from ethological studies of behavioral conflict.

3. Developing a robot model of action selection by the basal ganglia

The modeling work considered above serves to demonstrate signal selection by the basal ganglia rather than action selection per se. To show convincingly that the basal ganglia model is able to operate as an effective action selection device we believe it needs to be embedded in a real-time sensorimotor interaction with the physical world. An important goal has, therefore, been to construct an embedded basal ganglia model in which selection occurs between multiple, physically realized behaviors in a mobile robot. Since the use of robotics in computational neuroscience is relatively new, we preface our description of this model with a brief explanation of how we approach this task of embedding a computational neuroscience model within a robot architecture that generates observable behavior.

3.1. A methodology for embodied computational neuroscience

Any computational neuroscience model, robotic or otherwise, is composed of components that are 'biomimetic'—that is, they are intended to directly simulate neurobiological processes (at some appropriate level), and those that are merely 'engineered' so as to provide an interface that will allow the model to be interrogated and evaluated. The need for engineered components is particularly obvious in the case of robotic models where simulations of neural circuits must, at some point, be interfaced with (usually) very-non-neural robot hardware. Furthermore, in models that seek to simulate complete behavioural competences it is also generally impractical, because of the scale of the task, or impossible, because of the lack of the necessary neurobiological data, to simulate all components of the neural substrate for the target competence at a given level of detail. In this situation, engineered components are also required to substitute for the function of some of the neural circuits, known or non-known, that are involved in the production of that competence in an animal. In the current model, since the biological substrate of interest is the basal ganglia, the system components that provide the interface between the robot hardware (and low-level controllers) and the models of the basal ganglia and related nuclei have been constructed as a set of engineered sub-systems that we collectively denote as the *embedding architecture*. While broadly 'biologically inspired', we would stress that this embedding

architecture is not intended to directly mimic any specific neural substrate.

Latimer (1995) has identified the presence of two such distinct types of model components as a universal characteristic of Cognitive Science research. In his terminology, components that are intended to be biomimetic are said to be 'theory-relevant', and those that simply make the model useable are 'theory-irrelevant'. In fact, Latimer makes this distinction only to immediately deconstruct it! 'Theory relevance', after all, is largely in the eye of the beholder, and what, to one researcher, is a theory-irrelevant assumption made to get the simulation running, is to a critic, an unjustified fix on which the results of the model critically depend. Such issues have, for example, provided an important line of attack for detractors of connectionist models of psychological processes (see, e.g. Massaro, 1988; Pinker & Prince, 1988). Furthermore, whether a particular component of a model is deemed to be 'theory-relevant' or not, can depend as much on what hypothesis is being tested as on the nature of the model itself. Thus, whilst we would argue here that the specific details of how (robotic) motor behaviour is implemented is not relevant from the standpoint of the action selection hypothesis of basal ganglia function, such details would become relevant if the same model were to be evaluated as a theory of a complete sensorimotor loop.

Since the use of engineered components is unavoidable in Cognitive Science, but their 'theory-irrelevance' cannot be taken for granted, it is important: (i) that these elements of a model are described in sufficient detail to allow their evaluation and replication, (ii) that the interface with the inputs and outputs of the biomimetic components respects important biological constraints; and (iii) that where engineered components turn-out to have significant behavioural or functional consequences (i.e. are potentially theory-relevant) these are explored and, where possible, related to functional properties of relevant neural systems. In this article, we attempt all three tasks. First, in the remainder of this section, and in the appendices, we give a full description of the embedding architecture and demonstrate that, at a functional level, the decomposition of this architecture into behaviour-related (action) sub-systems is consistent with ethological evidence. Second, in Section 2 (above), we reviewed evidence justifying our general assumption that the inputs to the basal ganglia inputs encode action salience, and that its outputs act as gating signals that suppress undesired motor acts (we also revisit these issues in Section 5). Third, in Section 5.2, we will consider whether there are possible neural correlates for specific components of the embedding architecture that have significant functional consequences.

3.2. A model task

To evaluate the action selection properties of the embodied basal ganglia model requires an environment/task-setting complex enough to present interesting competitions between alternative behavior systems, yet simple enough to establish base-line levels of performance and to allow detailed analyses of the resulting patterns of behavior switching. In developing a task to meet these needs we were inspired by observing the behavior-switching of food-deprived rats placed in an unfamiliar rectangular arena containing a centrally located dish of food pellets (see Fig. 4, top). The initial behavior of such animals is typically exploratory, defensive, and characterized by avoidance of open space. Animals placed in the centre of the arena quickly move to the periphery, then tend to stay close to the arena walls, showing a preference for the corners of the arena, and little or no visible interest in food consumption. As the animal becomes more accustomed to the novel environment, hunger-related behaviors become more apparent. A common 'foraging' behavior being to locate the food dish, collect a food-pellet, and carry it back to a 'nest' corner of the arena (identified by the presence of bedding material) to be consumed. The balance between locomotion, feeding, and resting is of course sensitive to the level of hunger of the animal and its familiarity with the arena.

Our efforts to create a setting in which to test the embedded basal ganglia model have focused on producing

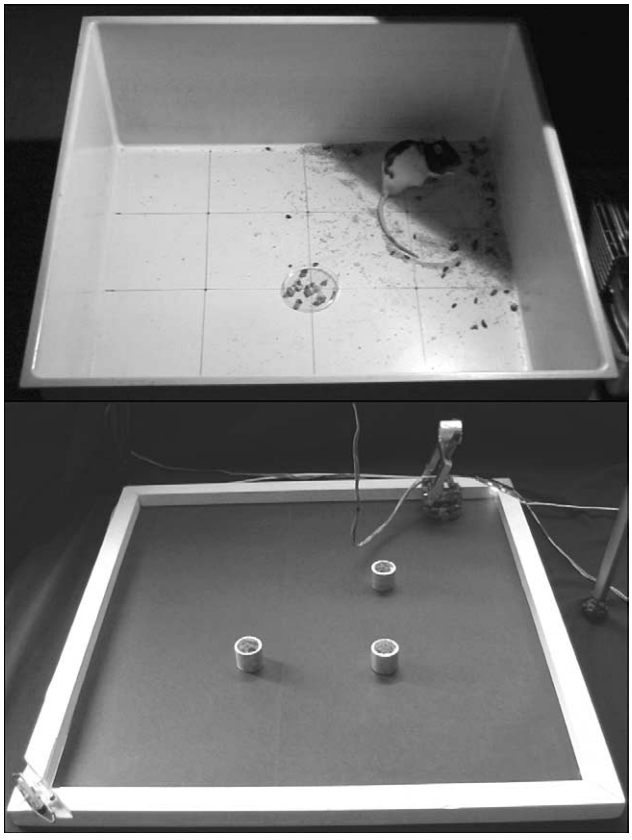

Fig. 4. The behavior of an adult rat in a square arena with a shaded nest area (top right) and central food resource (top) has provided the inspiration for the task setting investigated in the robot model of action selection by the basal ganglia (bottom).

a similar, if much simplified, problem setting for a small mobile robot. The robot is placed in a walled, square arena (55×55 cm^2) containing a number of small cylindrical objects (see Fig. 4, bottom). The cylinders substitute for food pellets, so the collection and consumption of food is modeled by collecting cylinders and depositing them in a 'nest' corner of the arena. The 'nest' is identified by the presence of a local light source (an 8v filament bulb) of which there are two, placed in diagonally opposite corners. Simulated motivations are used to modulate the robot's inclination to avoid open space ('fear'), and to collect cylinders ('hunger') through the time-course of each experiment.

3.3. The robot control architecture

The full robot control architecture is illustrated in Fig. 5, and the following sub-sections, together with the appendices, provide a full description the various components of this architecture. Fig. 5 distinguishes: (i) the robot and the primitive sensory and motor systems available to it, (ii) the *embedding architecture* that provides a repertoire of action (behavioral) sub-systems, computes their relative salience, and combines their outputs subject to gating by the basal ganglia, and (iii) the extended basal ganglia model that provides the substrate for resolving action selection conflicts. As noted above, it is only this third element of the model that aspires to mimic specific aspects of vertebrate brain function. Other components of the architecture that are included to satisfy the requirements for a working control system do, however, provide useful hypotheses concerning the embedding of the basal ganglia within the wider brain architecture, and we return to this issue in the discussion.

The robot control architecture has a large number of free parameters, that specify, for instance, the timings of sub-elements of behavior patterns (Section 3.3.2) and the weightings for action 'salience' calculations (Section 3.3.3). We have opted to use hand-tuned parameters throughout, as the free parameters in the embedding architecture do not need to be optimal but simply adequate to generate desired behaviour. This practise is consistent with much of the existing research on action selection where hand-coded systems are frequently employed (Maes, 1995). From the point of view of robot control, the capacity to learn from experience would clearly make our architecture more adaptive, however, the goal of the current study is limited to investigating the selection capabilities of an embodied basal ganglia model, so optimization of the embedding architecture is not a critical requirement.

3.3.1. The robot sensory and motor systems

The Khepera™ I is a small cylindrical robot, 60 mm in diameter, with two driven wheels and a detachable gripper arm. The robot senses the environment through an array of eight peripheral sensors, which can operate in both an active mode, as an infra-red proximity sense, and in a passive mode as an ambient light sense. In active mode, the sensor array has a very limited range, reliably detecting nearby vertical surfaces no further than 25 mm away. In this respect, it is somewhat analogous to a biological tactile sensory system, such as the rat vibrissae. In addition, the robot has a positional sensor on the gripper arm to determine whether it is currently raised or lowered, and

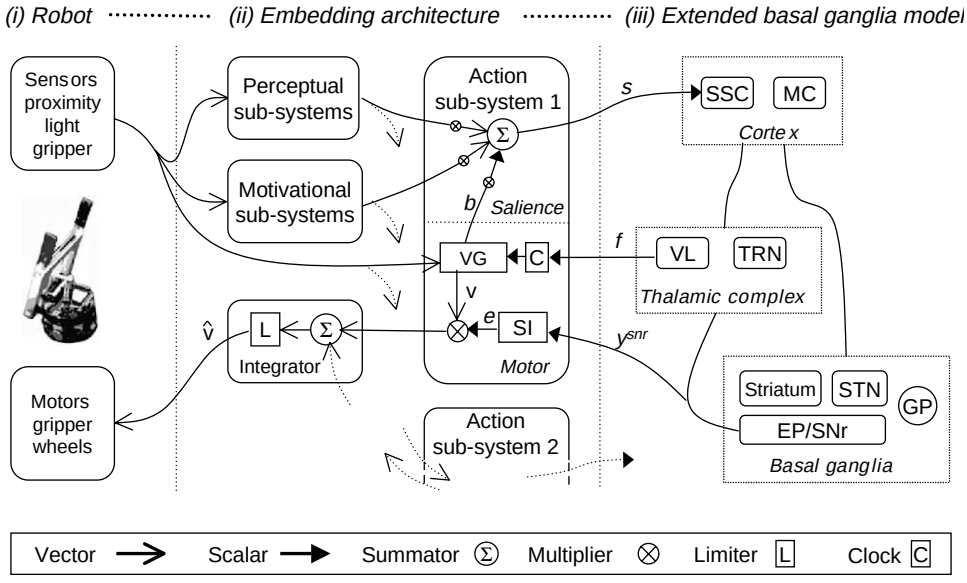

Fig. 5. The embedded basal ganglia model. The model is composed of three parts: (i) the robot and its sensory and motor primitives, (ii) the embedding architecture—a repertoire of perceptual, motivational, action (behavioral) sub-systems—and its interface to (iii) the biomimetic extended basal ganglia model (whose full connectivity is shown in Figs. 3, and 2c). Connections for the first of the five action sub-systems are shown (projections to and from other action sub-systems are indicated by dotted lines). Abbreviations: VG—(motor) vector generator, SI—shunting inhibition, *b*—busy signal, *s*—salience signal, *f*—feedback signal, y^{snr}—basal ganglia output, *e*—gating signal, v—motor vector, $\hat{\mathbf{v}}$—aggregate motor vector.

a binary-valued optical sensor that detects whether there is an object between the gripper jaws. Further details of the robot sensory systems are given in Appendix A. The two wheel motors can be independently driven forwards or backwards, and the gripper turret is powered by two motors, one to lift/lower the arm, the other to open/close the gripper. Further details of the motor systems are given in Appendix D. A serial link, controlled by *Webots* 2.0 robot interface software, is used to send sensor readings to, and receive motor commands from, the computer hosting the embedding architecture and basal ganglia model. This interface operates on a series of discrete time-steps providing updates at a rate of approximately 7 Hz. For convenience of notation, indexing according to the current 'robot time-step' is assumed in the following account of the embedding architecture (note, however, that the embedded basal ganglia model has a different intrinsic time-step as explained in Section 3.3.4 below).

3.3.2. The embedding architecture—action sub-systems

The control architecture of the robot includes five behaviors, or *action sub-systems*, which it can switch between at any time. These are: searching for cylinders (*cylinder-seek* or *Cs*), picking up a cylinder (*cylinder-pickup*, *Cp*), looking for a wall (*wall-seek*, *Ws*), following alongside a wall (*wall-follow*, *Wf*), and depositing the cylinder in a corner (*cylinder-deposit*, *Cd*). Each action sub-system operates independently to compute a stream of output signals that are directed toward the robot motor systems. So, for instance, *cylinder-seek* uses the infra-red proximity sense to detect nearby surfaces and to discriminate objects that are likely to be cylinders from other contours such as walls, and generates motor outputs that specify movement towards or away from the stimulus object as appropriate.

Our decomposition of robot activity into these five sub-systems is inspired by the ethological classification of behavior. Each action sub-system consists of a set of condition-action mappings, and three of the five action sub-systems—*cylinder-seek*, *wall-seek*, and *wall-follow*—map patterns of input from the peripheral sensor array into movements that orient the robot towards or away from specific types of stimuli (e.g. object contours). These behaviors can be viewed as belonging to the ethological category of *orienting responses* or *taxes* (see, e.g. Hinde, 1966). The two remaining sub-systems—*cylinder-pickup* and *cylinder-deposit*—generate stereotyped, and carefully timed, patterns of movement modeled on the ethological concept of a fixed action pattern (FAP). As originally defined by Lorenz (1935), FAPs are species-specific, instinctive responses to specific patterns of stimulation. Although a FAP may describe a complex spatio-temporal pattern of movement, a distinctive feature is that, once elicited, the overall form of the pattern (though not the parameters of specific motor elements) is uninfluenced by further external cues (Colgan, 1989). Perhaps the best known example of a FAP is the pattern for egg-retrieval, displayed by many ground-nesting birds, which has been described as having three sequential elements (Hinde, 1966; Tinbergen, 1951): (i) stand up, (ii) place the bill beyond the egg, (iii) roll the egg back into the nest (moving the bill from side-to-side to prevent the egg from slipping). By comparison, the fixed action pattern for *cylinder-pickup* in the robot model constitutes five sequential elements: (i) slowly approach the cylinder (to ensure correct identification and good alignment for pickup), (ii) back away (to allow room to lower the arm) whilst opening the gripper, (iii) lower the arm to floor level, (iv) close the gripper (hopefully around the cylinder), (v) return the arm to vertical. The term 'fixed action pattern' has been criticized within ethology for over-emphasizing the stereotyped and instinctive nature of the resulting behavior—'modal action pattern' (Barlow, 1977; Colgan, 1989) is, therefore, sometimes preferred. We have used the original term here both because our robot implementation of FAPs is consistent with Lorenz's definition, and because researchers in neuroethology have continued to find this a useful concept (Casseday & Covey, 1996; Ewert, 1987; Hoyle, 1984; McFarland & Bosser, 1993; Toates, 1998).

Whilst an action pattern may, in general, exploit sensory or proprioceptive data to shape ongoing motor output, some FAPs are held to be ballistic in nature (Ewert, 1987; Hinde, 1966), suggesting the involvement of intrinsic pattern-generating mechanisms. In the robot model, the relative paucity of appropriate sensory data has led us to investigate the use of such intrinsic patterning to regulate sequencing within a FAP. Specifically, the timing of the sub-elements of a pattern are determined relative to the state of an internal clock (C in Fig. 5) and the full behavior is implemented as a set of mappings from elapsed time, as recorded by this clock, to specified patterns of motor output. Given that the spatiotemporal organization of the robot FAP is regulated solely by this intrinsic time signal, a critical issue is how the sub-system clock is itself controlled. Our architecture here assigns an important role to the output of the basal ganglia by making the state of the clock depend upon thalamocortical feedback. Specifically, the sub-system clock is enabled (non-zero) only if there is a non-zero *feedback* signal from the VL thalamus in the relevant basal ganglia channel (indicated by the symbol *f* in Fig. 5). Since this aspect of the embedding architecture has a significant functional role (i.e. is potentially 'theory-relevant' with respect to the action selection hypothesis) we will consider evidence of a role for the basal ganglia in behavioural timing in our discussion (Section 5.2.2).

We designate v to be the vector generated by any given action sub-system that encodes its current motor output. To be effectively gated by the basal ganglia we require that all elements of v are positively valued and lie in the interval [0,1], and to interface with the *Khepera* robot we make v a nine-element vector containing a distributed

coding of the target left- and right- wheel-speeds (two elements each), arm-position (three elements), and gripper-position (two elements). Further details of this motor encoding scheme are given in Appendix B, which also provides a full description of the condition-action mappings implemented by each of the action sub-systems. The elements of the robot's behavioral repertoire are illustrated in Fig. 6.

3.3.3. The embedding architecture—determining salience

A centralized action selection system requires mechanisms that can assimilate relevant perceptual,

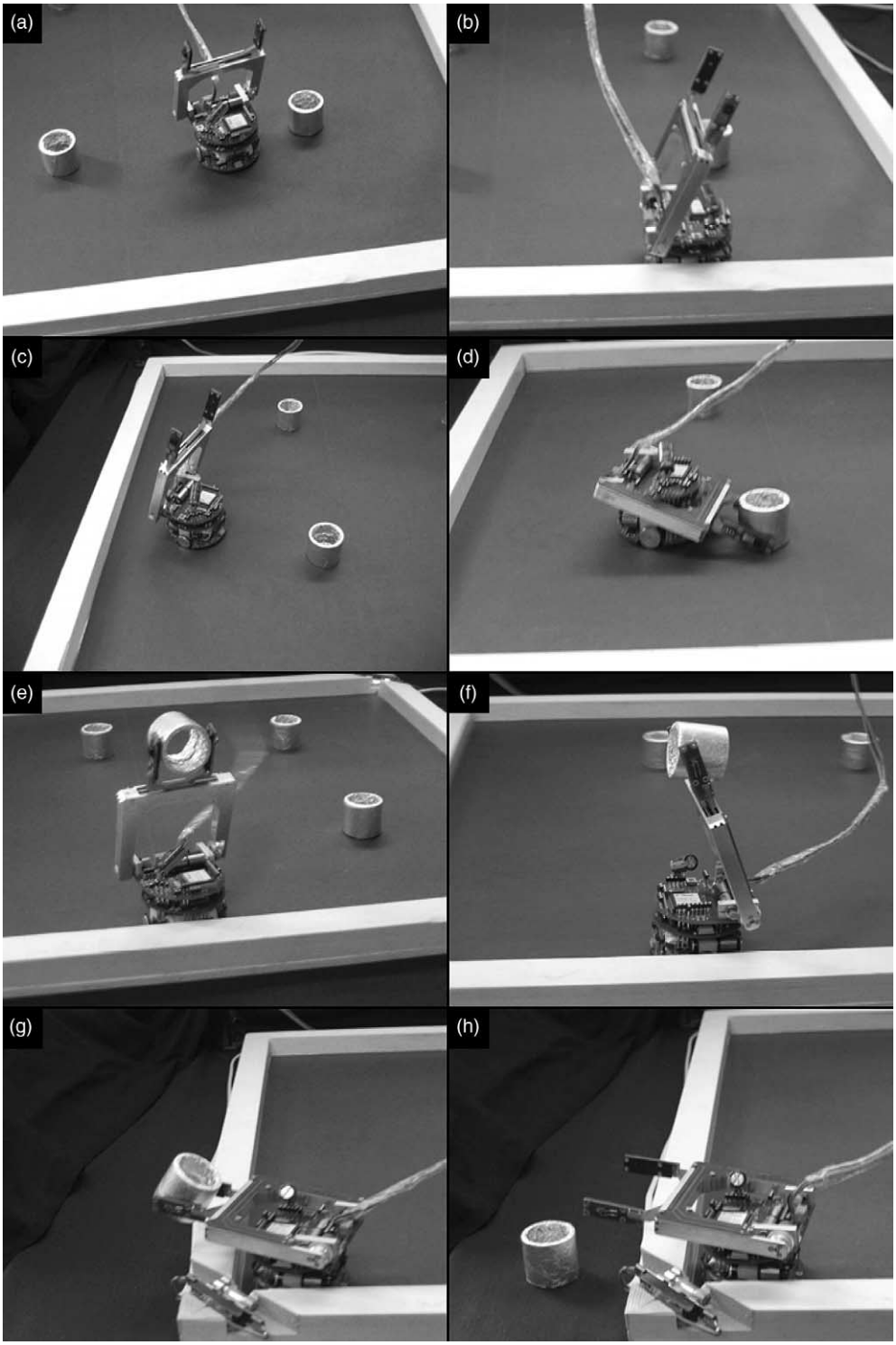

Fig. 6. Elements of robot behavior in the simulated foraging task: (a) *wall-seek*, (b) *wall-follow*, (c) *cylinder-seek,* (d) *cylinder-pickup*, (e) *wall-seek* (carrying a cylinder), (f) *wall-follow* (again carrying a cylinder), (g and h) *cylinder-deposit*.

motivational, and contextual signals to determine, in some form of 'common currency' the relative salience or urgency of each competing behavior (McFarland, 1989; Redgrave et al., 1999a). In the embedding architecture of our model, at each time-step, a salience value for each action sub-system is calculated as a weighted sum of relevant *perceptual* and *motivational* variables, and may also be dependant on the current activity status of the action sub-system itself. Each of these contributions to the salience calculation is briefly described below.

As ethologists have noted, the perceptual stimuli that give rise to a behavioral selection, often termed *sign stimuli*, are often quite different from those that are used to control the execution of the selected behavior (Colgan, 1989; Ewert, 1987). Sign stimuli, generally, indicate the presence (or absence) in the immediate environment of the relevant affordances for different behaviors. In the robot model, these values are computed by *perceptual sub-systems* from the raw sensory data available to the robot and generate four bipolar signals indicating: the presence (+1) or absence (−1) of a nearby wall (p_{wall}), nest (p_{nest}), or cylinder (p_{cyl}), or of an object in the robot gripper (p_{grip}).

An action selection mechanism also requires information about intrinsic state, indicating, for example, the current level of energy reserves (McFarland, 1989; McFarland & Bosser, 1993). In the current model, two simple intrinsic drives, loosely analogous to 'hunger' and 'fear', are calculated by two *motivational sub-systems*. 'Fear' (m_{fear}) is calculated as a function of exposure to the environment and is reduced with time spent in the environment, whilst 'hunger' (m_{hung}) gradually increases with time and is reduced when cylinders are deposited in the nest corners of the arena. Further details of the calculation of the perceptual and motivational variables are given in Appendix C.

In addition to perceptual and motivational input our model allows an action sub-system to contribute to its own salience computation by generating a signal indicating the urgency or importance attached to completing an ongoing task. We have adopted the term *busy signal* to describe a contribution to the weighted salience calculation that encodes this aspect of the activity status of an action sub-system (indicated by the symbol *b* in Fig. 5). In the robot model, such signals provide contributions to the salience calculations for three sub-systems. In *cylinder-pickup* a busy signal, b_{pick}, boosts the sub-system salience while the robot backs-up in order to grasp a target cylinder (the robot is generally unable to detect the cylinder during this maneuver), the busy signal then continues after the cylinder is grasped and until the robot arm is returned to a safe, vertical position. The role of the signal is to compensate for the salience changes that occur as the perceptual variables p_{cyl} (cylinder detection) p_{grip} (gripper status) switch sign during the task. In a similar fashion, *cylinder-deposit* uses a busy signal, b_{dep}, to boost its salience after the cylinder has been released and until the robot arm is returned to vertical. Finally, *wall-follow*, generates a signal, b_{foll}, if a nearby surface is detected by only one of its six proximity sensors. In this situation the wall percept, p_{wall}, often has a negative value (since there is insufficient sensory input to reliably identify a wall), so the signal encourages wall-following to be sustained until an unambiguous percept of the wall is regained or the robot loses track of the surface altogether. Full details of when each of these busy signals is generated are given in Appendix B. Some possible neural correlates of such signals are considered in Section 5.2.1.

The overall salience s_i for the ith action sub-system is a linear weighted sum (including a threshold term) of relevant perceptual and motivational variables and the busy signal (if required) for that sub-system. The weights given below were selected by hand to provide closely matched action selection competitions, then 'tuned' whilst observing the robot until the appropriate and opportunistic action selection was observed:

$$\text{cylinder} - \text{seek} : s_1 = s_{\text{seek}}$$
$$= -0.12p_{\text{cyl}} - 0.12p_{\text{grip}} - 0.06m_{\text{fear}} + 0.45m_{\text{hung}}$$

$$\text{cylinder} - \text{pickup} : s_2 = s_{\text{pick}}$$
$$= 0.21p_{\text{cyl}} - 0.15p_{\text{grip}} - 0.18m_{\text{fear}} + 0.18m_{\text{hung}} + 0.78b_{\text{pick}} + 0.25$$

$$\text{wall} - \text{seek} : s_3 = s_{\text{wall}}$$
$$= -0.12p_{\text{wall}} + 0.14p_{\text{grip}} + 0.18m_{\text{fear}} + 0.25$$

$$\text{wall} - \text{follow} : s_4 = s_{\text{foll}}$$
$$= 0.12p_{\text{wall}} + 0.14p_{\text{grip}} + 0.21p_{\text{fear}} + 0.25b_{\text{foll}} + 0.25$$

$$\text{cylinder} - \text{deposit} : s_5 = s_{\text{dep}}$$
$$= 0.33p_{\text{nest}} + 0.33p_{\text{grip}} + 0.18m_{\text{hung}} + 0.40b_{\text{dep}} + 0.13$$

These salience signals form the input to the model basal ganglia to which we turn next. The elements of the embedding architecture responsible for interfacing basal ganglia outputs with the motor system are then described in Section 3.3.5.

3.3.4. The extended basal ganglia model—a biomimetic substrate for action selection

In the robot, the task for the basal ganglia model is to arbitrate at each time-step between the five available action sub-systems and to generate a pattern of action selection over time that results in coherent sequences of behavior. For the experiments reported below, we used the model of basal ganglia intrinsic circuits described by

Gurney et al. (2001a,b) extended to include the models of VL thalamus and the thalamic reticular nucleus as described by Humphries and Gurney (2002). The full functional architecture of the model, therefore, combines the elements in Figs. 2c and 3.

In a living animal, the activity of the brain and of the body both unfold in continuous time, therefore, the ideal scenario for modeling would be to simulate both neural processes and behavioral processes at the same, high temporal rate. Unfortunately, the current robot model presents a problem in that the sense-act cycle operates in discrete steps at the relatively sedate pace of approximately 7 Hz. This raises the issue of how we relate the update rate of the basal ganglia model to that of the robot. In this study, we have chosen not to enforce a specific, fixed mapping between the two update cycles, as this could lead to artifacts caused by the intermittent sampling of basal ganglia activity at non-equilibrium values. Instead, we have opted to run the basal ganglia model to convergence at each robot time-step. Clearly, by allowing only equilibrium basal ganglia states to influence motor output we lose the opportunity to observe the behavioral consequences of basal ganglia dynamics at high temporal rates, a topic that merits future investigation in its own right.

For convenience, a brief summary of the full basal ganglia model is provided next; the reader is referred to Gurney et al. (2001a,b) and Humphries and Gurney (2002) for a detailed justification of its form.

The standard leaky integrator unit used throughout model is defined as follows. Let a be the unit activation and u be the *net input* (or total post-synaptic potential) generated by the afferent input to the unit. Given a rate constant k (corresponding to the cell membrane capacitance and resistance) $\dot{a} = \mathrm{d}a/\mathrm{d}t$ is given by:

$$\dot{a} = -k(a-u) \tag{1}$$

The output y of the unit, which corresponding to the mean firing rate, is bounded below by 0 and above by 1, and is given by the piecewise linear function:

$$y = L(a,\theta) = \begin{cases} 0, & a < \theta \\ (a-\theta), & \theta \le a \le 1/(1+\theta) \\ 1, & a > (1+\theta) \end{cases}. \tag{2}$$

Note that θ is the threshold below which any value outputs zero—a negative threshold value, therefore, indicates tonic activation, whilst a positive value indicates resistance to synaptic input.

The following equations specify the net input u_i and output y_i for the ith channel in each component of the model. The net input u_i is computed using the outputs y_i of other components of the model except for the model somatosensory cortex where it is equal to the current salience input, s_i, for that channel (see Section 3.3.3). Dopamine modulation of the model is provided by introducing a multiplicative factor in the equations specifying afferent input to the striatum—in striatal D1 channels where dopamine modulation increases synaptic efficacy the effective weight is $(1+\lambda)$ where $0 \le \lambda \le 1$, in D2 channels, where the effect is to reduce efficacy, the weight is $(1-\lambda)$. All parameter and threshold values are the same as those used in Gurney et al. (2001a,b) and Humphries and Gurney (2002), except the weighting of the inputs from the TRN to the VL thalamus[1]. Note that, since the architecture forms a continuous loop, definition of the net input for the motor cortex requires the output of VL thalamus (y_i^{vl}) defined later in the list. All other values are defined consecutively:

$$\text{Somatosensory cortex(ssc)}: \; u_i^{\mathrm{ssc}} = s_i, \; y_i^{\mathrm{ssc}} = L(a_i^{\mathrm{ssc}}, 0.0). \tag{3}$$

$$\text{Motor cortex(mc)}: \; u_i^{\mathrm{mc}} = y^{\mathrm{ssc}} + y_i^{\mathrm{vl}}, \; y_i^{\mathrm{mc}} = L(a_i^{\mathrm{mc}}, 0.0).$$

$$\text{Striatum D1}(d1): \; u_i^{d1} = (1+\lambda)1/2(y_i^{\mathrm{ssc}} + y_i^{\mathrm{mc}}),$$

$$y_i^{d1} = L(a_i^{d1}, 0.2).$$

$$\text{Striatum D2}(d2): \; u_i^{d2} = (1-\lambda)1/2(y_i^{\mathrm{ssc}} + y_i^{\mathrm{mc}}),$$

$$y_i^{d2} = L(a_i^{d2}, 0.2).$$

$$\text{Subthalamic nucleus(stn)}: \; u_i^{\mathrm{stn}} = 1/2(y_i^{\mathrm{ssc}} + y_i^{\mathrm{mc}}) - y_i^{\mathrm{gp}},$$

$$y_i^{\mathrm{stn}} = L(a_i^{\mathrm{stn}}, -0.25).$$

$$\text{Globus pallidus(gp)}: \; u_i^{gp} = 0.9\sum_i y_i^{\mathrm{stn}} - y_i^{d2},$$

$$y_i^{\mathrm{gp}} = L(a_i^{\mathrm{gp}}, -0.2).$$

$$\text{EP/SNr(snr)}: \; u_i^{\mathrm{snr}} = 0.9\sum_i y_i^{\mathrm{stn}} - y_i^{d1} - 0.3y_i^{\mathrm{gp}},$$

$$y_i^{\mathrm{snr}} = L(a_i^{\mathrm{snr}}, -0.2).$$

$$\text{VL Thalamus(vl)}:$$

$$u_i^{\mathrm{vl}} = y_i^{\mathrm{mc}} - y_i^{\mathrm{snr}} - \left(0.125y_i^{\mathrm{trn}} + 0.4\sum_{j \ne i} y_j^{\mathrm{trn}}\right),$$

$$y_i^{\mathrm{vl}} = L(a_i^{\mathrm{vl}}, 0.0).$$

$$\text{Thalamic reticular nucleus (trn)}:$$

$$u_i^{\mathrm{trn}} = y_i^{\mathrm{mc}} + y_i^{\mathrm{vl}} - 0.2y_i^{\mathrm{snr}}, \; y_i^{\mathrm{trn}} = L(a_i^{\mathrm{trn}}, 0.0).$$

[1] Lower weights are used on the TRN-VL connections than in the previous article, as the original weights generated some instabilities in architectures with three or more active channels.

In the robot implementation, the time-course of the basal ganglia model is simulated using a Euler solution[2] to Eq. (1):

$$\Delta a_i(t) = -k(a_i(t-1) - u_i(t))\Delta t, a_i(t) = a_i(t) + \Delta a_i(t). \quad (4)$$

Hence the net input $u_i(t)$ is calculated using the outputs $y_i(t-1)$ of other model components from the previous iteration step and the salience s_i which is fixed for the current robot time-step (and therefore throughout convergence). The output $y_i(t)$ is obtained by substituting $a_i(t)$ in Eq. (2) with the appropriate threshold. A rate constant $k=25$, and step-size $\Delta t=0.012$ were used in the experiments reported here, and the model was considered to have converged whenever the smallest Δa on two consecutive time-steps was less than 0.0001.

Previous studies (Gurney et al, 2001b; Humphries and Gurney, 2002) have established that the basal ganglia model shows good selection properties, across a wide-range of salience pairings, with the simulated dopamine level set at $\lambda=0.2$. This value was, therefore, used in all this experiments described in the current article; the consequences of variation of the simulated dopamine level will be investigated in detail in a separate article.

3.3.5. The embedding architecture—gating motor output

The output of the model basal ganglia gates the motor vector produced by each action sub-system by reducing or increasing the inhibition on the corresponding motor pathway. This is implemented in our embedding architecture using a gating signal e generated using a *shunting inhibition* mechanism (labeled *SI* in Fig. 5) defined such that, for the ith action sub-system, e_i $(0 \leq e_i \leq 1)$ is given by:

$$e_i = L(1 - y_i^{\text{snr}}/y_{\text{tc}}^{\text{snr}}, 0.0). \quad (5)$$

Here $y_{\text{tc}}^{\text{snr}}$ is a constant equal to the tonic output of EP/SNr obtained when the model is run to convergence with zero salience input on all channels. For the parameters of the basal ganglia model listed above $y_{\text{tc}}^{\text{snr}} = 0.169$. Our model assumes that this level of basal ganglia output provides complete inhibition of target structures, and that disinhibition of targets begins when the output falls below $y_{\text{tc}}^{\text{snr}}$, increases linearly with decreasing output, and is maximal when the output reaches zero. Since this element of the embedding architecture mediates the effects of basal ganglia output on the motor system it plays a 'theory-relevant' role in our model. We will, therefore, consider evidence, in Section 5.2.3, that basal ganglia output to motor and pre-motor systems may also have a gating effect similar to shunting inhibition.

The gated motor outputs of all action sub-systems are summed over all channels and the result passed through a further limiter to give the aggregate vector:

$$\hat{\mathbf{v}} = L\left(\sum_i e_i \mathbf{v}_i, 0.0\right). \quad (6)$$

Finally, the motor plant maps the vector $\hat{\mathbf{v}}$ into motor commands that can be understood by the robot, details of this mapping are given in Appendix B.

Note that the aggregate motor vector expresses target values for the motor state, that is, target wheel-speeds, gripper-arm elevation, and gripper-jaw position. In the event of full basal ganglia inhibition of all channels, this aggregate command will have zero value and the robot will freeze in its current position. In the event that one or more channels is partially (but not fully) disinhibited, the robot will act but its movements may be slowed by the resulting reduction in the size of the motor signals. Finally, note that the motor signal generated by any losing behavior that is not fully inhibited by the basal ganglia will be combined with that of the winner. This mechanism allows for the possibility of *distortion* (the robot tries to do two things at once) in the event of ineffective suppression of competitors by the basal ganglia.

3.3.6. Time course of the robot model

To make clear the relationship between the update cycle of the robot, the embedding architecture, and the basal ganglia model, the activity in the embodied model occurring in one robot time-step can be summarized as follows:

(i) Enact the robot's current aggregate motor command $\hat{\mathbf{v}}$ and obtain new sensor data.
(ii) For each action sub-system i update the salience s_i and generate a new motor vector v_i.
(iii) Run the basal ganglia model to convergence.
(iv) Using the output, y_i^{snr}, of the converged basal ganglia model generate the gating signal e_i and compute a new aggregate motor command $\hat{\mathbf{v}}$.
(v) Using the output of the VL thalamus, y_i^{vl}, enable or disable the sub-system clock of any sub-system that implements a fixed action pattern.

For the embedded basal ganglia model, the activation values of all leaky integrator units at convergence are retained as the starting values for the next time-step. This allows for the possibility of hysteresis across robot time-steps and has potentially important consequences for behavior.

[2] The Euler method is known to have stability problems if the time-step chosen is too large. However, with a small enough time-step it is sufficiently accurate and less computationally expensive than some other methods (an important consideration in developing robot models that must make decisions in finite time). In the light of the known stability issues our algorithm was extensively tested to ensure that the time-step chosen was small enough to avoid stability issues. The behaviour of the model used in the robot was also tested on several benchmark runs against a simulation, implemented in Simulink™, using a fixed-step Dormand–Prince (5th order) solver with a time-step of 0.01 and the outputs were found to be equivalent.

3.4. Action selection metrics

To assist the presentation of the model results it is helpful to define a number of terms to describe the outcomes of action selection competitions.

First, we note that the gating signal e_i, defined in Eq. (5), provides a useful normalized measure of selection by the embedded basal ganglia model. In evaluating the performance of the model we will, therefore, use e_i as a measure of the *efficiency* with which the motor output of the ith action sub-system is transmitted to the motor resource. Allowing a 5% margin from absolute limits, we define the selection state of the ith competitor as *fully selected* if $0.95 \leq e_i \leq 1$, *partially selected* if $0.05 \leq e_i < 0.95$, and *unselected* if $e_i < 0.05$.

It is helpful to have specific metrics relating to the winning sub-system, hence, we define

$$e_w = \max_{\forall i} e_i \tag{7}$$

as the efficiency of the winner(s) in the current robot time-step, and

$$d_{\mathrm{w}} = \frac{2\left(\sum_i e_i - e_{\mathrm{w}}\right)}{\sum_i e_i} \tag{8}$$

to be the level of distortion affecting the output of the winner(s). Note that d_w will equal zero when all other competitors have zero efficiency, will increase with the number of partially disinhibited losers, and will be 1.0 or greater if two or more channels are fully disinhibited. Finally, inspired by ethological research (Lehner, 1996), we describe an uninterrupted series of time-steps that share the same winner(s), and for which $e_{\mathrm{w}} \neq 0$, as a single *bout* of behavior.

The result of the basal ganglia selection competition, as a whole, can be described by the vector e. Using the criteria just defined for single competitors we assign the following labels to the possible outcomes of the full competition:

Clean selection. One competitor fully selected, all others unselected.
Partial selection. One or more competitors partially selected, no competitor fully selected.
Distorted selection. One competitor only fully selected, at least one other partially selected.
Multiple selection. Two or more competitors fully selected.
No selection. All competitors unselected.

4. Experiments

Three experiments were performed using the basal ganglia model. Experiment 1 (Section 4.1) was designed to aid the interpretation of the behavior of the robot model and employed a systematic search of a salience space using a disembodied version of the extended basal ganglia model. Experiment 2 (Section 4.2) was our main investigation of a robot model implemented using the hand-tuned salience inputs described in Section 3.3.3. Experiment 3 (Section 4.3) investigated the behavioral consequences of using multiple, high salience inputs in the robot model.

4.1. Experiment 1—selection properties of the disembodied model

4.1.1. Method

To provide a framework for interpreting the behavior of the robot model, we performed a systematic search of a salience space using a disembodied version of the extended basal ganglia model. Specifically, we simulated a five-channel model, with two active channels, varying the salience s_1 in channel 1 systematically from 0 to 1 in steps of 0.01, then for each value of channel 1 salience, varying the salience s_2 of channel 2 from 0 through 1, again in steps of 0.01. For each resulting salience vector (s_1,s_2,0,0,0) the model was run to convergence and the result classified according to the scheme set out in Section 3.4. Importantly, selection competitions were run in sequence from low values to high values. The activations levels of all leaky integrators in the model were initialized to zero for each new value of s_1 but thereafter, while that salience value was tested, were retained from one competition to the next. In other words, we simulated the situation where channel 1 was initially the only active channel, and gradually increased channel 2 while holding channel 1 constant, the goal being to simulate some aspects of the continuity of experience of the robot model in which the recent history of basal ganglia selection competitions may influence the current competition through hysteresis.

4.1.2. Results

The disembodied model displayed a high-proportion of clean selections (79%), with some partial selections (17%). Reduced selection efficiency and distortion occurred only for evenly matched, high salience competitions. The model also showed evidence of hysteresis that varied with salience intensity.

The state-space search described above resulted in 10,000 (100×100) salience competitions of which 78.6% resulted in clean selection, 16.7% in partial selection, 4.3% in no selection, 0.3% in distorted selection, and 0% in multiple selection. Some further results from this analysis are shown in Fig. 7. In the upper graph, we show the efficiency, e_{w}, of the winning channel for each salience competition plotted in the (s_1,s_2) plane, and below this the equivalent plot for distortion, d_{w}, of the winning channel. Progressively lighter shading indicates, respectively, increasing efficiency (top) and decreasing distortion (bottom). The dotted line in the upper graph also indicates the boundary below which the selection

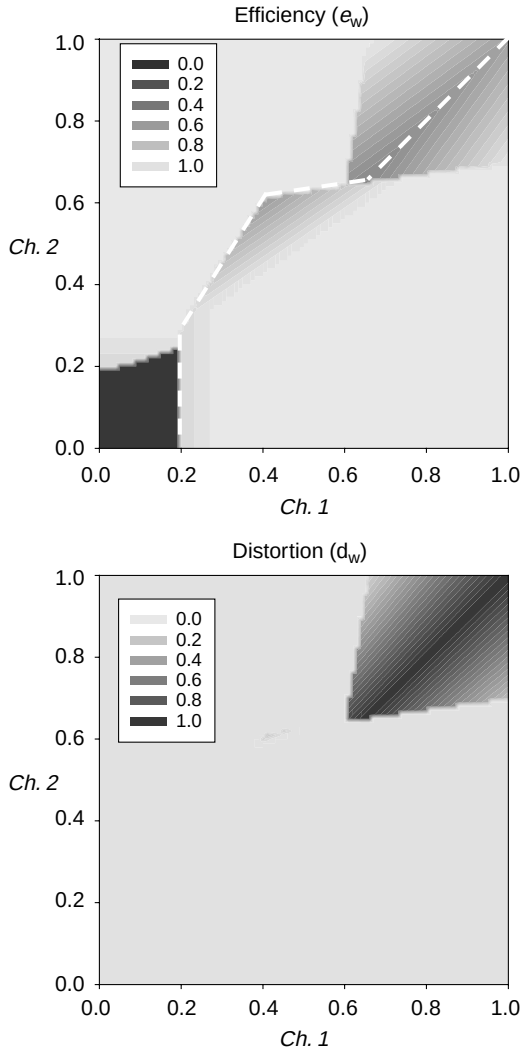

Fig. 7. Efficiency (top) and distortion (bottom) in the winning channel, for a systematic salience-space search with two active channels. Progressively lighter shades show higher efficiency (top) or reduced distortion (bottom). The salience space was sampled at a resolution of 0.01. For each salience value of channel 1, channel 2 began at 0 and increased gradually. The model was re-initialized only when a new channel 1 value was selected thus allowing the possibility of hysteresis. The dotted line in the upper graph indicates the boundary below which the selection competition was resolved in favor of channel 1.

competition was resolved in favor of channel 1 (i.e. channel 1 efficiency exceeds that of channel 2). Several properties of Fig. 7 are worthy of comment. First there was high efficiency, minimal distortion, and hence clean selection, across most of the state space. Second, there was no selection only for very low salience pairings. Third, there was reduced efficiency of selection and significant distortion for strong, evenly matched, salience values (s_1,$s_2 > 0.6$), resulting in partial selection in this area of the state-space. Finally, we note that the model showed significant hysteresis (as indicated by the dotted line in the upper graph). In particular, a salience value between 0.2 and 0.6 in channel 1 was able to resist a 'rising tide' of channel 2 salience until the latter was substantially stronger in numerical terms. Furthermore, changes in the overall intensity of the salience competition resulted in different levels of hysteresis, with the effect most pronounced at intermediate levels of salience.

4.2. Experiment 2—the robot basal ganglia

4.2.1. Method

The robot was tested for five trials, each lasting 300 s (2000 robot time-steps), with all parameters of the model as described in Section 3.3. The experimental procedure was as follows. At the start of each trial the robot was placed in the centre of the arena (see Fig. 4) facing one of the four walls, with four cylinders placed 18 cm diagonally in from each corner. All motor outputs were initially set to zero, and the basal ganglia model run to convergence with zero salience on all channels. For each trial automatic logs were generated detailing the robot's sensory, motivational, and basal ganglia state, at each robot time-step, and the overall bout structure of its behavioral selections. Most trials were also recorded in digital video, using a camera positioned approximately 1 m above the arena, to allow detailed examination of the robot's behavior and its interaction with objects and surfaces in the environment.

4.2.2. Results

In the following we describe: (i) the general selection properties of the robot model, (ii) the intrinsic processing in the model basal ganglia during robot behavior, and (iii) the observed behavior of the robot model.

4.2.2.1. The robot engaged in a high proportion of closely fought selection competitions resulting in predominantly clean selections (84%). Hysteresis, which generates behavioral persistence, was exhibited in 10.1% of competitions.

Fig. 8 provides a partial view of the salience space explored by the robot. Each cell shows the proportion of the (approximately 10,000) basal ganglia competitions (1 per robot time-step) for which the salience of the winning channel (horizontal-axis) and that of the *most salient loser* (vertical-axis) fell within a given range (note, there was also, typically, non-zero salience in other losing channels that is not shown in the figure) with darker colors indicating greater proportions. The plot shows that there were a large proportion of closely fought salience competitions, but that the area of high salience competitions (where reduced efficiency can be expected) was relatively sparsely sampled. Our analysis again classified the outcome of the basal ganglia selection competition, at each time-step, according to the criteria specified in 3.4. Across all five trials, 84.4% of salience competitions resulted in clean selection, 9.7% in partial selection, and 5.9% in no selection. There was no distorted selection or multiple channel selection. This result indicates that the range of operation within which the basal ganglia model generates (primarily) clean selection is

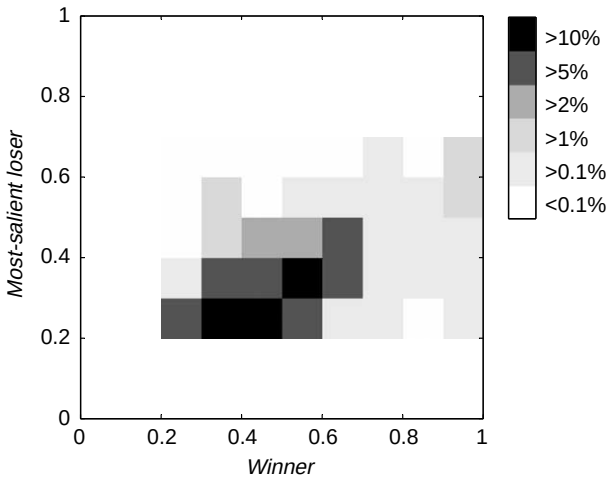

Fig. 8. A partial view of the salience space sampled by the robot in a typical trial. Axes denote the salience of the winning channel (horizontal), and of the most salient loser (vertical). Shading indicates the proportion (darker = greater) of the approximately 10,000 salience pairs falling within a given (0.1 × 0.1) bin. Average channel salience was 0.235 (across all channels and all time-steps), the average winning salience 0.475, and the average margin (between winner and most salient loser) 0.154.

sufficient to meet the action selection requirements of a reasonably complex robotic task.

The presence of some shaded cells above the diagonal ($x = y$) in Fig. 8 provides evidence of hysteresis in the embedded basal ganglia model (i.e. competitions for which the winning channel has lower salience than its closest competitor). In the robot, hysteresis translates into behavioral persistence, where the robot continues to display a selected behavior beyond the point where a *winner-takes-all* selector would switch to a higher salience task. Over all five trials, persistence was shown on 10.1% of time-steps and therefore had a significant influence on the observed behavior of the robot.

4.2.2.2. Intrinsic processing in the embodied model. Fig. 9 illustrates some of the intrinsic processing occurring in the embedded basal ganglia model during the first 180s (approximately 1200 robot time-steps) of a typical trial. Fig. 9a shows, for each channel (action sub-system), activity in two of the basal ganglia input structures—the somato-sensory cortex, y^{ssc} (solid line), whose output is proportional to the net salience, and the D1 striatum, y^{d1} (dotted line). The final plot in 9a shows the cortical output for the winning channel (solid line) compared with that of the most salient loser (dotted line). Fig. 9b shows the model activity, per channel, for the basal ganglia output nuclei EP/SNr, y^{snr}. The final plot in 9b showing average EP/SNr output across the four losing channels (solid line) compared with that of the winning channel (dotted line). In the following, we briefly relate some key features of model intrinsic processing to computational properties of the basal ganglia model and embedding architecture, and to the observed behavior of the robot. We also present some quantitative measures relating the selection behavior of the embedded model to intrinsic activity in EP/SNr and STN.

Striatal activity reflected changes in channel salience, modulated by thalamocortical feedback. The graphs of cortical and striatal D1 activity (9a) show that the saliences varied both gradually and sharply with time reflecting changes in either the continuous, and generally slow-varying, motivations or the discrete and rapidly varying perceptual variables. The difference between the cortical and striatal activity (the filled and dotted lines) illustrates the effect of thalamocortical feedback in boosting selected channels, and of the striatal thresholds in suppressing low salience inputs. A period of no selection occurred in this trial during the interval $t = 160$–180 s where the cortical output of the most active channel was at a low level (< 0.3), there was a near-equal level of output in a second channel (see the final plot in 9a), and significant, non-zero output in two further channels. This outcome demonstrates that the threshold for selection is often higher in the five-channel robot model than in the two-channel, disembodied model illustrated in Fig. 7. This result is consistent with a previous finding (Gurney et al., 2001b) that the presence of multiple active channels makes the selection of any given channel more difficult, a property of the model that we have termed 'selection limiting'.

'Busy signals' performed a significant role in maintaining behavioral selections. The utility of a sub-system busy signal for maintaining a selected behavior is also visible in the graphs of cortical and striatal output (9a). For instance, during *cylinder-pickup* there is a noticeable change partway through the execution of the behavior ($t = 75$–79s) corresponding to the moment when the primary objective of grasping the cylinder was achieved. The busy signal was engaged at this point to maintain the salience of the behavior above that of its competitors while the full movement (returning the robot arm to vertical) was completed. Without this signal the salience of the behavior would have fallen more substantially once the cylinder was gripped, resulting in failure to complete the full action pattern. In other words, the busy signal allowed the maintenance of the behavior while an essential 'house-keeping' element of the task was completed. A busy signal played a similar role during the execution of *cylinder-deposit* ($t = 83$-87s). The action of the busy signal during *wall-follow* can be seen in the series of intermittent salience spikes ($t = 5$–40s) that compensated for temporary interruptions of the wall percept and, therefore, prevented an early return to wall-seeking behavior. In this role, the busy signal helped avoid unnecessary behavior switching due to noisy or ambiguous sense data.

Basal ganglia output showed, predominantly, full disinhibition of winners and increased inhibition of losers. Average EP/SNr activity increased during behavioral selections. The graphs of basal ganglia output (9b) show the consequences of the further intrinsic basal ganglia selection mechanisms (feed-forward off-centre on-surround,

and the GP control circuit) that resulted in sharp decision boundaries between action sub-systems with selected sub-systems fully disinhibited (zero EP/SNr output). Note that there is a marked difference in the mean activity of losing channels (see bottom graph) during the period when there was no selected behavior ($t=160$–180s), as compared with all times at which there was a winning behavior. To quantify this effect, average EP/SNr activity was calculated across all five runs for different selection outcomes. Taking the EP/SNr output during periods of no selection as a baseline, average output for all channels (losing channels) was 123% (134%) of baseline during periods of partial selection, and 156% (182%) during clean selection. More generally, across all selection competitions, there was a strong negative correlation ($r=-0.895$) between the activity of the winning channel and the average activity in losing channels. Thus as a winning channel was disinhibited, the level of inhibitory output to losing channels increased.

STN activity increased during behavioral selections and was the principle cause of increased inhibition of losing channels. In the basal ganglia model, the only structure providing excitatory input to EP/SNr is the STN which consequently showed a high correlation ($r=0.884$) with activity in losing channels. STN is itself driven by cortical inputs (somatosensory and motor) encoding channel salience and thalamocortical feedback (EP/SNr-VL-MC), and by a recurrent loop with GP. Analysis of STN firing in the model indicates that this showed gradual increases with cortical activity relating to increased salience ($r=0.696$, with SSC), and also showed a sharp increase when the baseline periods of no selection were compared with either partial selection (176% of baseline), or clean selection (272%). From this data, we can conclude that while selection of a winning channel generates, through thalamo-cortical feedback, increased inhibition of EP/SNr of that channel (via the direct striatonigral pathway), the same

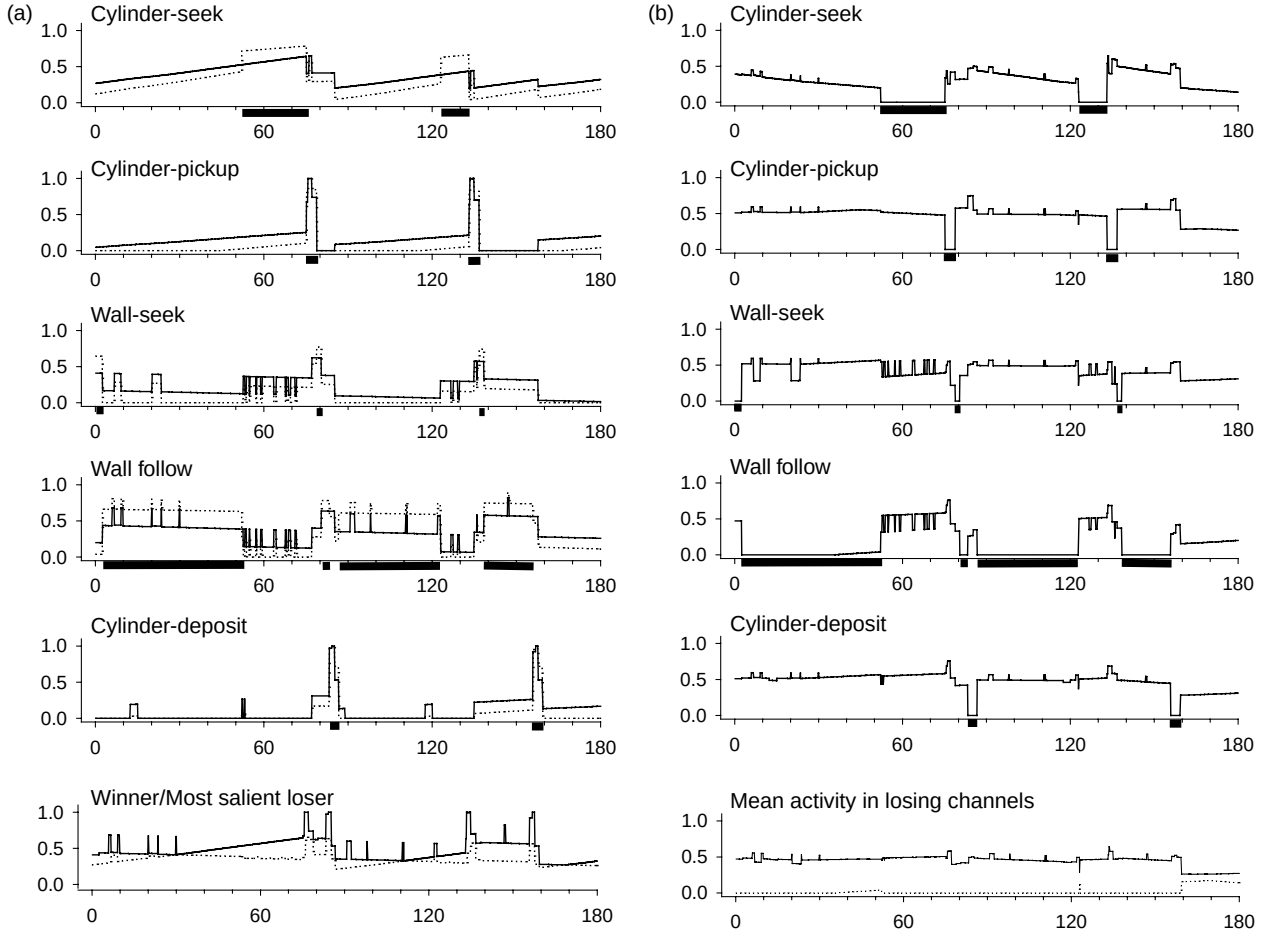

Fig. 9. Intrinsic activity of the embedded basal ganglia model for the first 180s of a typical trial. (a, left) The first five graphs show, for each of the five basal ganglia channels, the output of the somatosensory cortex, y^{ssc} (solid line), and of the D1 striatum, y^{d1} (dotted line) plotted against time. The final plot shows the y^{ssc} output of the winning channel (solid line) compared to that of the most salient loser (dotted line). (b, right) The first five graphs show the per-channel output of EP/SNr, y^{snr}, while the final plot shows the average y^{snr} output of losing channels (solid line), compared to that of the winning channel (dotted line). Solid bars below the sub-system plots indicate periods of full selection of the corresponding action sub-system. Note that there is no selection during the period $t=160$–180 s.

positive feedback signal also leads, via STN, to increased EP/SNr activity in losing channels.

4.2.2.3. The observed behavior of the robot showed clean and decisive switching between selected channels, was organized in extended bouts and goal-achieving sequences, and displayed variability in sequence structure and duration. Based on our earlier definition of a behavioral bout, the activity of the robot (as illustrated in Fig. 9) can be seen to consist of appropriate, and suitably extended bouts of individual activities that are integrated over time into appropriate, higher-order *sequences* of goal-achieving behavior. This bout/sequence structure is more easily seen in Fig. 10 where we show sub-system activity for the full 300s of the trial for which sample basal ganglia activity was shown in Fig. 9. From the top down, the first five graphs in this figure show the efficiency e of each of the five action sub-systems over time, with bouts of full selection appearing as solid blocks (in the style of a behavioral ethogram). The next (sixth) graph shows a plot of $(1-e_w)$ over time, and thus displays the extent to which the robot was expressing its current action inefficiently or engaging in periods of inactivity (note, that there was no distorted selection in this trial, therefore a plot of distortion is unnecessary). The next plot shows the structure of the robot behavior in terms of higher-order behavioral sequences, while the final plot shows the two simulated motivations. Selection of each action sub-system was triggered by relevant perceptual affordances, maintained for an appropriate period, and followed by rapid and decisive switching to the next bout. Behavior switching occurred whenever the salience of the ongoing activity fell significantly below that of a competitor, or the salience of a competitor rose significantly above that of the currently selected act. In either case, the ongoing behavior terminated abruptly and the new activity commenced with little delay (usually in the next robot time-step). The initial bout sequence—finding a wall (*wall-seek*) and then following it (*wall-follow*)—reflected the high initial level of simulated 'fear' and can be viewed as forming a higher-order sequence of *avoidance* (*Av*) behavior, that kept the robot away from open space. As 'fear' reduced and 'hunger' increased this was followed by a second episode of behavioral selections—finding and collecting a cylinder (*cylinder-seek*, *cylinder-pickup*), carrying it to a 'nest' (*wall-seek*, *wall-follow*) and dropping it there (*cylinder-deposit*)—that can be viewed as a sequence of appetitive or *foraging* (*Fo*) activity. The robot subsequently engaged in further sequences of avoidance and foraging interspersed with short periods of inactivity, where the robot displayed no movement, corresponding to times at which both artificial motivation levels were low.

The model behavior illustrated in Fig. 10 is typical of that observed in all five trials, however, there are a number of factors that contributed to significant variability both within and across trials. These included small variations in the initial position of the robot and of the cylinders; sensor noise; perceptual aliasing (for instance ambiguous signals that could derive from either walls or cylinders); wheel slip; and friction against the arena floor and walls. Some of the effects of this variability are illustrated in Table 1 which depicts the transition frequencies for all behavioral pairs (preceding behavior on the vertical axis, subsequent behavior on the horizontal axis). The predominance of the "standard" foraging sequence—*Cs*, *Cp*, *Ws*, *Wf*, *Cd*—is clearly visible from high proportion of transitions lying on the diagonal. The *Cd–Wf* and *Wf–Cs* transitions reflect the occurrence of wall-following as an avoidance behavior subsequent to, or preceding, foraging. The smaller number of *Cp–Cs* transitions and *Wf–Ws* reflect the fact that the

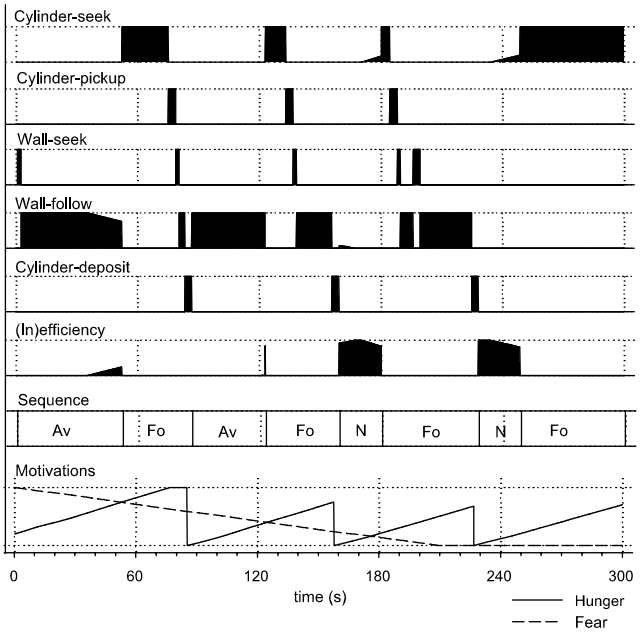

Fig. 10. Bout/sequence structure of action selection in the robot model for a full 300 s trial. From the top down, the first five graphs show the efficiency (e) of selection for a given action sub-system plotted against time, the sixth the inefficiency $(1-e_w)$ of the current winner, the seventh the higher-order structure of the bout sequences, (Av, avoidance; Fo, foraging), and the final graph the levels of the two simulated motivations. All measures vary between 0 and 1 on the y-axis. The robot began this trial with a high level of simulated 'fear' that resulted in higher salience for *wall-seek* than for other actions. After quickly finding a wall ($t=3$s), *wall-follow,* became more salient and was selected. These two bouts form a higher-order sequence of *avoidance* behavior. Avoidance behavior was interrupted by an increase in 'hunger' and decrease in 'fear' driving up the relative salience of *cylinder-seek*. Once the salience for *wall-follow* fell significantly below that of *cylinder-seek* the robot switched to the latter ($t=52$ s). When it found a cylinder, *cylinder-pickup* was selected ($t=75$ s), followed by *wall-seek* ($t=79$ s, this time carrying a cylinder), *wall-follow* ($t=81$ s), and finally *cylinder-deposit* ($t=84$ s) when a 'nest' area was detected. These four bouts constitute a sequence of appetitive or *foraging* (*fo*) activity. Having completed a foraging sequence the level of simulated 'hunger' fell to zero temporarily ($t=87$ s), and the robot engaged in a new period of avoidance (*wall-follow*, since the robot was already at the periphery of the arena). Increasing 'hunger' then led to three further sequences of foraging (the final one unfinished) interspersed by two periods of inactivity (as 'fear' approaches zero there was no motivation to perform avoidance behaviors).

Table 1
For each action sub-system the table shows the mean number of bouts per trial, the relative frequencies of alternative behaviors, and the relative frequencies of different transitions (preceding behavior on the vertical axis, subsequent behavior on the horizontal axis)

	Bouts per trial	Relative frequency %	Transition frequency %					
			Cs	Cp	Ws	Wf	Cd	No
Cs	3.6	15.0	0.0	**100.0**	0.0	0.0	0.0	0.0
Cp	3.6	15.0	16.7	0.0	**83.3**	0.0	0.0	0.0
Ws	5.2	21.7	0.0	0.0	0.0	**100.0**	0.0	0.0
Wf	6.6	27.5	30.3	0.0	18.2	0.0	**45.5**	6.1
Cd	3.0	12.5	0.0	0.0	0.0	46.7	0.0	**53.3**
No	2.0	8.3	100.0	0.0	0.0	0.0	0.0	0.0

No indicates a bout of inactivity. The transition matrix is dominated by the standard foraging sequence *Cs–Cp–Ws–Wf–Cd* (shown in bold type).

robot occasionally failed to grasp a cylinder correctly (and therefore returned to cylinder-seeking), or lost touch with the wall during *wall-follow* (and therefore returned to wall-seeking). A second consequence of variability is that there was a wide distribution of durations for foraging sequences (range 23.7–126.4s, median 36.63s), due, in part, to the simplistic search strategy employed by the robot and the short-range of its sensors.

4.3. Experiment 3—behavior of robot model when faced with high salience competitions

4.3.1. Method. We previously noted (Section 4.1) that a breakdown of clean selection can occur in the disembodied model when two competitors have high salience levels. To examine the behavioral consequences of this pattern of selection, the robot model was tested over five trials of 120s (approximately 800 robot time-steps) in which the salience of every channel was increased, on every time-step, by a constant amount (+0.4). All other aspects of the experimental procedure were as described for experiment 2 (Section 4.2).

4.3.2. Results

During a continuous sequence of high salience competitions the robot exhibited patterns of behavioral disintegration characterized by: (i) reduced efficiency and distortion of a selected behavior, and (ii) rapid switching and incomplete foraging behavior.

Fig. 11 shows the effect of increased salience intensity on exploration of the winner/most-salient-loser salience-space over all trials. The graph demonstrates that virtually all (∼4000) salience competitions appeared in the region of salience space (compare with Fig. 7) where reduced efficiency and distorted selection can be expected.

Fig. 12 illustrates the behavior of the robot in a typical trial. The initial avoidance sequence followed the expected pattern but the transition to foraging activity did not begin cleanly, instead showing reduced efficiency and intermittent, partial selection of (losing) avoidance behaviors. To the observer the movement of the robot behavior during the transition appeared somewhat slowed and 'tentative'. During the foraging bout there was an extended period of rapid switching between *cylinder-seek* and *cylinder-pickup* with the robot repeatedly approaching the cylinder but failing to grasp it. The pattern initially observed (t=60–85s) was for the robot to approach the cylinder; back up as if to collect it in the gripper; then move forward without lowering the gripper-arm, pushing the cylinder forward slightly. Later (t=85–90s, 110–115s), where both behaviors showed some partial selection, the robot would lower the arm whilst moving forward but fail to grasp the cylinder due to being incorrectly aligned.

In all five trials, the selection behavior of the robot was similarly inefficient and distorted with the robot frequently displaying rapid alternation of foraging acts. This is illustrated in the transition matrix in Table 2, which shows that the behavior of the robot was dominated by the sequence *Cs–Cp–Cs–Cp…* with no trials leading to a successful foraging sequence.

4.3.2.1. Rapid switching between foraging acts constitutes a 'behavioral trap' arising through errors in behavior

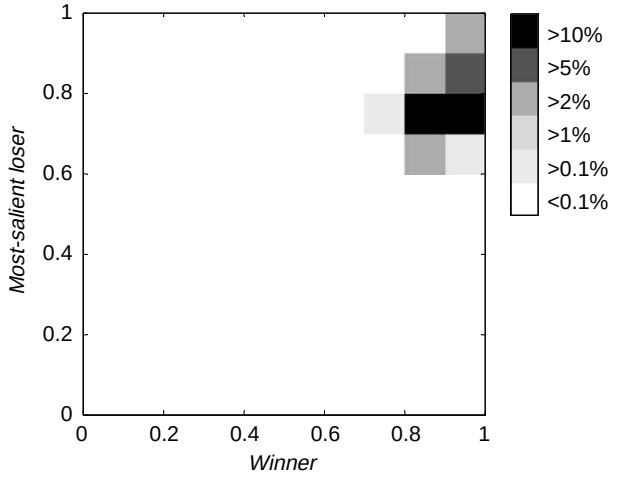

Fig. 11. Salience space exploration following a uniform (+0.4) increase in salience across all channels. Axes denote the salience of the winning channel (horizontal), and of the most salient loser (vertical). Shading indicates the proportion (darker=greater) of the approximately 4000 salience pairs falling within a given (0.1×0.1) bin. Average channel salience was 0.576 (across all channels and all time-steps), the average winning salience 0.935, and the average margin (between winner and most salient loser) 0.173.

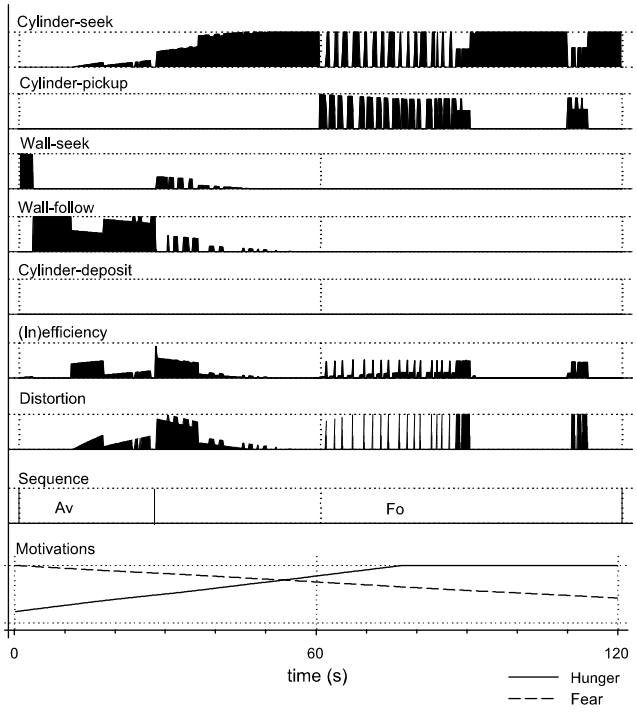

Fig. 12. Bout/sequence structure of action selection in the robot model for a trial of 120 s following a uniform increase (+0.4) in salience across all channels. From the top down, the first five graphs show the efficiency (e) of selection for a given action sub-system plotted against time, the sixth and seventh the inefficiency ($1-e_w$) and distortion (d_w) of the current winner, the eighth the higher-order structure of the bout sequences (Av, avoidance, Fo, foraging), and the final graph the levels of the two simulated motivations. All measures vary between 0 and 1 on the y-axis. The initial avoidance sequence followed the expected pattern with *wall-seek* succeeded by a period of *wall-follow*, however, the gradual increase in cylinder-seek salience, from approximately $t=15$ s onwards, caused reduced efficiency of the *wall-follow* behavior resulting in visibly slowed movement. The transition to foraging activity occurred at around $t=30$ s, *cylinder-seek* was selected but at reduced efficiency with intermittent partial selection of avoidance behaviors (*wall-seek*, *wall-follow*). When the robot found a cylinder ($t=60$ s) the *cylinder-pickup* behavior was cleanly selected but then interrupted prematurely—the robot backed-up ready to lower the gripper-arm but then suddenly switched back to *cylinder-seek*. There then followed a period of rapid switching between *cylinder-pickup* and *cylinder-seek* with the robot repeatedly approaching the cylinder but failing to grasp it. As the hunger motivation increased further, the robot displayed a mixture of both behaviors (*cylinder-seek* and *cylinder-pickup*) (around $t=90$ and 110 s) but at reduced efficiency, still failing to grasp the cylinder correctly.

maintenance.. The reduced efficiency and distorted selection that occurs with very high salience competitions is generally consistent with the analysis presented in Fig. 7. However, the disintegration observed in the foraging sequence—oscillation between two foraging behaviors while failing to grasp the cylinder—requires some further explanation. Recall that the *cylinder-pickup* FAP makes use of a busy signal at the point where the robot has backed-up to make room for the gripper arm and is consequently no longer able to detect the cylinder. In normal circumstances, this signal would be sufficient to maintain behavioral selection until the cylinder has been collected and the gripper arm raised to vertical. In the high salience model, however, the disappearance of the cylinder, which increases the salience of *cylinder-seek*, initiates a brief period of distorted selection (note the brief spikes in the graph of the distortion measure in Fig. 12), during which *cylinder-pickup* and *cylinder-seek* are simultaneously selected. High levels of distortion have an interesting consequence in the extended basal ganglia model, which is to reduce thalamocortical feedback on the winning channel (*cylinder-pickup*). This occurs because reduced SNr activity in losing channels generates increased TRN activity for those channels, which then inhibits the VL thalamus activity of the winner (see Fig. 3 and Section 3.3.4). In the model, the timing of the *cylinder-pickup* pattern, and thus of the busy signal, relies on continued thalamocortical feedback. When this feedback is lost, the sub-system clock is disengaged and the busy signal cancelled. The salience of *cylinder-pickup* then falls sharply, and the competing behavior, *cylinder-seek,* wins the subsequent basal ganglia selection competition. This pattern is then repeated when the robot re-establishes contact with the cylinder. In sum, the disintegrated pattern of rapid behavioral switching arises through the premature interruption of a behavior that depends upon an intrinsic salience boost (the busy signal) for its completion. This can be characterized as an error of *behavior maintenance*. The failure to execute the action pattern successfully (and thus to trigger subsequent elements of the behavioral sequence) places the robot in a 'behavioral trap' where it repeatedly executes an incomplete and ineffective sequence of actions.

5. Discussion

5.1. Summary of main findings

The embedded basal ganglia succeeded in generating sequences of integrated behavior in a robot model provided with a repertoire of alternative behaviors and varying levels of simulated motivations. The robot switched cleanly and decisively between successive behaviors, interrupting an ongoing behavior whenever there was a competitor with significantly higher salience. This outcome supports the hypothesis that the functional properties of basal ganglia circuitry (to the extent that they are captured by our computational model) make it suited to the task of resolving selection conflicts. The robot model, therefore, supports the claim of effective *action* selection by the basal ganglia, over and above earlier demonstrations of the good *signal* selection properties of these circuits. Whilst the model has an operating range that supports clean selection for most levels of salience competition, and is sufficient to provide appropriate selection in our robot task, reduced selection efficiency and partial selection of losing competitors can

Table 2
For each action sub-system the table shows the mean number of bouts per trial, the relative frequencies of alternative behaviors, and the relative frequencies of different transitions (preceding behavior on the vertical axis, subsequent behavior on the horizontal axis)

	Bouts per trial	Relative frequency %	Transition frequency %					
			Cs	Cp	Ws	Wf	Cd	No
Cs	14.6	**44.5**	0.0	**98.6**	0.0	1.4	0.0	0.0
Cp	14.4	**43.9**	**100.0**	0.0	0.0	0.0	0.0	0.0
Ws	1.8	5.5	0.0	0.0	0.0	100.0	0.0	0.0
Wf	2.0	6.1	60.0	0.0	40.0	0.0	0.0	0.0
Cd	0.0	0.0	0.0	0.0	0.0	0.0	0.0	0.0
No	0.0	0.0	0.0	0.0	0.0	0.0	0.0	0.0

No indicates a bout of inactivity. The transition matrix is dominated by switching between cylinder-pickup (*Cs*) and cylinder-seek (*Cs*) (bout and transition frequencies highlighted in bold type).

occur when the model is presented with multiple high-salience competitors. Hence, when a version of the model was tested with substantially increased salience across all channels, distorted motor output and behavioral disintegration were observed.

In the remainder of this discussion we consider: (i) some elements of the embedding architecture and their possible neural correlates, (ii) comparisons of the results from the robot model with neuroethological observations of animal behavior, and (iii) the relationship of the current study to other computational models of the basal ganglia.

5.2. Possible neural correlates of the robot embedding architecture

As previously noted (Section 3.1), our approach to developing a robotic test of the hypothesis that the basal ganglia performs action selection is based on the assumption that informative models can be constructed by combining biomimetic components (here the extended basal ganglia model) with sufficient engineered components to create a full working model. This strategy requires, however, that we devise a suitable interface between the biomimetic and engineered components such that appropriate input signals are supplied to the embedded neural model, and a biologically plausible role is assigned to its outputs. We have also argued that it is necessary to assess the engineered components of the model so-constructed with respect to their possible consequences for the theoretical issues under investigation. The following briefly considers key elements of the architecture/model interface with regard to these requirements.

5.2.1. Basal ganglia input encodes signals relevant to the selection and maintenance of ongoing behavior

The hypothesis that the basal ganglia is involved in selecting actions implies that the inputs to the basal ganglia encode the relative *salience* of competing actions (Redgrave et al., 1999a; Zink, Pagnoni, Martin, Dhamala, & Berns, 2003). Amongst the evidence lending weight to this view are studies showing activity in striatal spiny neurons just prior to movements (see Mink, 1996 for review). Our proposal that the basal ganglia is an action selection device makes the further claim, however, that basal ganglia activity is important not just for *selecting* winning actions but also for the appropriate *maintenance* and termination of selected actions (Redgrave et al., 1999a). That the basal ganglia is involved in the maintenance of selection is suggested by data showing that a substantial proportion of striatal projection neurons fire *after* movement has been initiated, and that the timing of this movement-related activity in the striatum is distributed over a wide-range of delays relative to the onset of movement (Aldridge, Anderson, & Murphy, 1980; DeLong, Alexander, Georgopoulos, Crutcher, Mitchell and Richardson, 1984; Jaeger, Gilman, & Aldridge, 1995; Mink, 1996). The inhibition of activity in basal ganglia output neurons (EP/SNr or GPi/SNr in primates) has similarly been recorded as occurring during the execution of limb movements (Mink & Thach, 1991; Schultz, 1986), saccades (Basso & Wurtz, 2002; Handel & Glimcher, 1999; Hikosaka & Wurtz, 1989), and behavioral bouts (Joseph, Boussaoud, & Biguer, 1985). The robot model we have described here, highlights a key issue in the appropriate maintenance of behavioral selections which is that the perceptual and motivational conditions that lead to the selection of a given behavior often do not persist for the full duration of the performance of that behavior. This means that a mechanism, such as *winner-takes-all*, that ignores the recent history of selection and allocates control of the motor system to the action sub-system with the highest instantaneous salience will be prone to *errors of behavior maintenance* such as the premature interruption of an ongoing behavior, or ‘dithering’ (rapid switching) between two actions with similar salience. Two logically possible solutions for this problem are: (i) that a winning competitor instigates some form of ‘mutual exclusion lock’ that prevents rivals from accessing motor resources until the intended motor act has been completed (and then releases the lock), or (ii) that the ongoing selection contest is biased in favor of the currently winning

competitor allowing it to maintain an 'edge' over its selection rivals, for an appropriately extended period, at lower (extrinsic) salience levels than were required to initiate it. Whilst a type (i) solution is often employed in real-time computer operating systems (Ganssle & Barr, 2003), our model proposes that the basal ganglia implements a type (ii) solution to the maintenance problem by providing additional salience support to the current winner for the duration of the behavior. More specifically, we have proposed two such salience-incrementing mechanisms. First, we have suggested that basal ganglia-thalamocortical loops instantiate a positive feedback circuit that can provide a significant salience boost to a winning sub-system (Redgrave et al., 1999a). In the extended basal ganglia model this feedback induces significant hysteresis (see Fig. 7), and thus generates behavioral *persistence* in the robot. Second, we have found that accurate control over the maintenance and termination of selection for action patterns may be best achieved when an action sub-system is able to generate a precisely timed, intrinsically generated contribution to its own salience, that we have termed a *busy signal*. We, therefore, hypothesize that basal ganglia activity during ongoing behavior may reflect in part, the operation of similar selection maintenance mechanisms.

The suggestion that basal ganglia thalamocortical loops act to generate increased salience in currently selected channels is consistent with a significant corpus of research in ethology indicating a role for positive feedback mechanisms in the maintenance of behavioral selections (Houston & Sumida, 1985; McFarland, 1989; Roeder, 1975). The further notion, that signals generated by ongoing motor activity can be important for maintaining behavioral selections, might explain why the input to the basal ganglia, from both cortical (Cowan & Wilson, 1994; Levesque, Charara, Gagnon, Parent, & Deschenes, 1996) and subcortical (Chevalier & Deniau, 1984; Krout, Loewy, Westby, & Redgrave, 2001) sources, often comprises collateral branches from fibers projecting to motor regions of the brainstem and spinal cord. At the current time there is no agreed interpretation of these data, the busy signal employed in our robot model, therefore, suggests a novel hypothesis concerning a possible functional role for these motor-related inputs.

Note that while our model invokes a single leaky integrator in each nucleus for each channel, this is intended to represent a population of neurons in each target structure. Thus, in considering the striatum, for example, our model is consistent with the possibility that different sub-populations of striatal neurons encode different aspects of the salience of the current selection at different times during the execution of a motor act. In other words, some sub-populations of striatal neurons may be specifically concerned with the initiation of behavior (and thus fire before behavior onset), and others with the maintenance of the current selection (and thus fire during the expression of the behavior).

It is interesting to contrast the type (ii) maintenance mechanisms implemented in our model (and hypothesized for the basal ganglia), that will allow an interrupt by a much stronger competitor, with the type (i) 'mutual exclusion lock', or *mutex*, preferred in real-time operating systems. Interestingly, the use of a *mutex* can lead to a resource allocation problem termed 'priority inversion', that occurred most famously in the significant computer difficulties experienced by the 1997 Mars pathfinder mission (Reeves, 1998). Whilst there are workarounds that can avoid the inversion problem these are computationally non-trivial involving, for instance, the inheritance of priority levels from one task to another (Sha, Rajkumar, & Lehoczky, 1990). It is, therefore, conceivable that 'softer' forms of resource locking, such as the maintenance mechanisms described here, could have applications in artificial scheduling systems.

5.2.2. Thalamocortical feedback may play a role in timing sequential action patterns

A role for the basal ganglia in behavioral timing is consistent with our general hypothesis that the basal ganglia regulate the maintenance and appropriate termination of action as part of the solution to the overall action selection problem. Our robot model invokes the use of the output of VL thalamus as a signal regulating the internal clock used by each action sub-system that generates an intrinsically patterned behavioral sequence (i.e. a fixed action pattern). Although the manner in which basal ganglia output is used to control these intrinsic patterning systems is not intended to be closely biomimetic, the following evidence supports the suggestion that thalamocortical feedback is important for behavioral timing. First, cortico-basal ganglia-thalamocortical loops have been specifically hypothesized as a likely neural substrate for interval timing (Meck, 1983; Meck & Benson, 2002), and have been the basis for a neurobiologically plausible computational model (Matell & Meck, 2000). Second, dopaminergic drugs have been found to affect the speed of the 'internal clock' (Buhusi & Meck, 2002), further implicating the basal ganglia as part of the functional brain system for time estimation. Finally, the timing of repetitive, intrinsically generated sequences (such as paced finger-tapping) is known to be impaired in Parkinson's patients with reduced thalamic activity a possible causal factor (Elsinger, Rao, Zimbelman, Reynolds, Blindauer and Hoffmann, 2003; Marsden & Obeso, 1994). Meck and co-workers (Gibbon, Church, & Meck, 1984; Meck & Benson, 2002) have elaborated a number of models of the role of the basal ganglia in interval timing, the simplest of which, we propose, bears interesting similarities to the mechanism we have used in our model. Specifically, Gibbon et al. (1984) have suggested: (i) that the basal ganglia can act as a form

of 'switch' that can be opened or closed depending on the detection of temporally significant information, (ii) that when closed this switch allows the flow of pacemaker pulses to target systems; and (iii) that when the temporally significant information ended, the switch opens stopping the flow of pulses. Similarily, in our model, the internal clock of a target FAP sub-system is enabled (i.e. begins to measure elapsed time from zero) by basal ganglia disinhibition (closing the switch) and is disabled (reset to zero) when the output for that basal ganglia channel returns above threshold (opening the switch). Whilst the robot model would benefit from the inclusion of a more biologically realistic simulation of interval timing it is likely that this will require modeling of populations of oscillating neurons (Matell & Meck, 2000) rather than the simpler rate-coding units used currently.

As noted above, our robot embedding architecture allows winning sub-systems to reinforce their own salience during critical passages of behavior. Where this additional salience input is triggered by the internal clock, it is logical to suppose that the loss of thalamocortical feedback, and consequent disruption of sub-system timing, should also interrupt the busy signal as implemented in the model.

5.2.3. Basal ganglia output to the brainstem may operate as a motor gating signal

Computational studies have suggested that the position of axon terminals on the dendritic tree of a target neuron help determine the extent to which inhibitory inputs have non-linear effects. More specifically, terminals on or close to the cell body have been proposed to have a non-linear, multiplicative 'shunting' effect that scales incoming excitatory signals (Blomfield, 1974; Koch, Poggio, & Torre, 1983). Our robot model instantiates such a form of shunting inhibition for the influence of basal output nuclei on motor pattern generators via the gating signal e (Eq. (5)). GABAergic terminals have been viewed as implementing shunting inhibition elsewhere in the nervous system (Ulrich, 2003), and this interpretation of the role of GABAergic basal ganglia outputs to the brainstem motor systems appears to be consistent with the available, if limited, electron microscopy evidence. For instance, Tsumori & Yasui (1997) found SNr axon terminals on the soma and proximal dendrites of neurons in the rat superior colliculus, while Shink, Sidibe, & Smith (1997) found that GPi output to the pedunculopontine nucleus in the squirrel monkey formed symmetrical contacts predominantly with proximal dendrites. Since, the action selection hypothesis asserts that the basal ganglia act to gate access to the final motor path we might expect to find further evidence of shunting inhibition in future studies of EP/SNr output to motor and pre-motor systems.

5.3. Comparisons with ethological and neuroethological investigations of animal behavior

5.3.1. Action selection and behavioral sequencing

In our robotic task, the embedded model of the basal ganglia demonstrates the capacity to generate extended sequences of appropriate and goal-directed behavior, organized at two temporal scales— bouts (*cylinder-seek*, *cylinder-pickup*, etc.) and behavioral sequences (*avoidance*, *foraging*). This outcome accords with a variety of studies in which the vertebrate basal ganglia have been shown to play a role in generating sequential behavior. For instance, Kermadi and co-workers (Kermadi & Boussaoud, 1995; Kermadi & Joseph, 1995) have found caudate nucleus activity in monkeys, linked to memorized sequences of saccades and arm movements. Berridge and co-workers (Aldridge & Berridge, 1998; Cromwell & Berridge, 1996; Meyer-Luehmann, Thompson, Berridge, & Aldridge, 2002) have shown that the striatum is necessary for the expression of species-typical sequences of grooming behavior in rodents, and have recorded related activity in dorsolateral and ventromedial striatum and in substantia nigra. Electrophysiological studies in behaving animals have also identified activity encoding successive phases of maze-traversing behavior in the rat ventral striatum (Mulder, Tabuchi, & Wiener, 2004; Shibata, Mulder, Trullier, & Wiener, 2001) and dorsal striatum (Schmitzer-Torbert & Redish, 2004). Finally, behavioral sequences in non-mammalian vertebrates, such as the toad prey-catching sequence studied by Ewert and co-workers (Ewert, 1987; Ewert, Buxbaum-Conradi, Dreisvogt, Glagow, Merkel-Harff & Rottgen, 2001), may also be subserved by basal ganglia loops that are largely homologous to those found in mammals (Marin, Gonzalez, & Smeets, 1997; Redgrave et al., 1999a).

Our experiments with the robot model raise some interesting questions with regard to this neurobehavioral data on basal ganglia sequencing, which are best illustrated with reference to the research on rodent grooming by Berridge and co-workers (Aldridge & Berridge, 1998; Cromwell & Berridge, 1996). Grooming patterns in rodents often appear in a stereotypic sequence that Aldridge and Berridge (1998) have described as a "four-phase syntactic chain". Whilst the grooming pattern itself is thought to be generated outside the basal ganglia (see below) its behavioral expression has been shown to be critically dependent on the integrity of a small area of the anterior dorsolateral striatum. In electrophysiological single-cell recordings from behaving animals (Aldridge and Berridge, 1998), activity in dorsolateral striatal neurons showed marked increases during one or two phases of the grooming sequence. In addition, the majority of these neurons did not respond when similar grooming movements were made outside a sequence (suggesting that their activity is sequence-related not movement-related). Finally, some neurons in ventromedial striatum, where lesions do not

impair the production of syntactic grooming chains, also showed increased activity during grooming sequences, however, these increases were smaller than those seen in the dorsolateral striatum. The intrinsic activity of the robot basal ganglia model, as shown in the traces of model 'D1' units in Fig. 9a, suggests that activity in striatal neurons can occur in multiple channels simultaneously, with correlated changes occurring in those channels whose salience is based on over-lapping feature sets. However, it is generally only the most active channel whose motor output is gated for behavioral expression (see simulated EP/SNr output in Fig. 9b). Applied to the data from the grooming study, this suggests that the (weaker) activity of ventromedial striatal neurons may code for losing behaviors that are partially primed by contextual salience cues present during the sequence of syntactic grooming. A related hypothesis can also be formulated with respect to the activity in those dorsolateral neurons that fire during multiple phases of grooming syntax. Specifically, it seems plausible that a neuron tuned to fire maximally in a single phase of grooming, might also show activity during an earlier or later phase due to a partial overlap in afferent input (related to shared contextual cues) with the neurons coding for the other phase. Again, this activity will not feed-through to behavioral expression, since activity in weaker channels loses out during the resolution of the competition elsewhere in the basal ganglia. Several examples of this can be seen in Fig. 9a, for instance, the *wall-seek* channel shows strong activity ($t=77$–79s) during the preceding *cylinder-pickup* (as well as some activity during *wall-follow*) whilst the *cylinder-deposit* channel shows a significant activity during the preceding bout of *wall-follow* ($t=80$–83s)—in all cases the corresponding small reductions in EP/SNr output are insufficient to allow these channels to distort the behavioral expression of the winner. Note, the hypothesis that multi-phase activity in dorsolateral striatal neurons is due to overlapping feature sets differs from the suggestion put forward by Aldridge and Berridge (1998) that neurons that fire during multiple phases code "serial order as a higher-order property distributed over the duration of the chain" (p. 2784).

Whilst the activity of our robot model shows interesting parallels with experimental studies in mammals, at a purely behavioral level, the most obvious similarity is perhaps with the behavior of an amphibian—the prey-capture sequence of the toad *bufo bufo*, which has been carefully described and analyzed by Ewert (1987). Toad prey-catching is composed of a sequence of action patterns—orienting to the prey (*o*), approaching (*a*), fixating (*f*), and snapping (*s*)—that may be implemented in the toad brain by disinhibitory loops involving the ventral striatum (Ewert et al., 2001). Summarizing an extensive series of experiments on prey-catching behavior Ewert concludes that "it is not the previous action, but the ongoing stimulus situation ⟨…⟩ that determines the subsequent response" (Ewert, 1987, p. 340). Much the same can be said of our robot model, where it is primarily the perceptual/motivational context that determines which behavior is selected at any given moment. Further, although 'standard' toad prey-catching behavior is described by the action sequence *o*, *a*, *f*, *s*; observed behavior often departs from this template in a manner that demonstrates both flexibility and opportunism. Thus, "if the distance between prey and toad is short, prey-catching consists of *o*, *f*, *s*; if prey suddenly appears close to the animal, only, *o*, *s*, or *f, s,* or just *s* is elicited; if the prey flees the toad's appetitive pursuit response occurs—depending on the prey's behavior—in variable succession such as *o*, *o*, *o*, *a*, *o*, *a*, *f*, *a*, *f*, *o*, *f*, *s*" (Ewert, 1987, p. 340). The behavioral sequences generated by the robot are similarly context dependent. So, for instance, the 'standard foraging sequence'—*Cs*, *Cp*, *Ws*, *Wf*, *Cd*—may be emerge as *Cs*, *Cp*, *Cs*, *Cp*, *Ws*, *Wf*, *Cd*, if the robot fails to grasp the cylinder correctly on first attempt, or as *Cs*, *Cp*, *Ws*, *Cd*, if wall-seeking behavior fortuitously places the robot in the 'nest' area.

Whilst the two-level structure of robot behavior is suggestive of hierarchical organization, it is clear from the design of our embedding architecture that the observed behavioral sequences are not the consequence of any explicit hierarchical decomposition of control. Rather, robot activity is organized by a stream of moment-to-moment action selection 'decisions' structured by the robot's perceptual and motor interactions with its environment, by its internal (motivational) state, and by the selection/switching properties of the embedded basal ganglia model. We conclude, following Ewert (1987), that hierarchical organization of control is not essential for the appearance of sequential activity. This is not to say that we would rule out the possibility of hierarchical organization in vertebrate action selection. Indeed we have argued (Prescott et al., 1999; Redgrave et al., 1999a) that the part closed-loop, part open-loop inter-relationships between the different basal ganglia domains (limbic, associative, and motor) (Joel & Weiner, 1994) strongly suggest some form of hierarchical decomposition of control, the benefits of which have been identified by research in artificial agents (Bryson, 2000; Prescott et al., 1999). Instead, the robot model makes clear that any account of animal behavior that purports to show hierarchical decomposition must demonstrate that emergent sequencing, of the kind described here, is not a viable alternative explanation.

A related issue concerns the granularity of the action selection provided by the basal ganglia. For instance, some researchers have proposed a role for the basal ganglia in a more fine-grained sequencing of movement than selecting between competing behavioral alternatives (see Mink, 1996 for review). Indeed, this level of action selection would be equivalent to the type of movement sequencing currently performed within our fixed action pattern sub-systems (e.g. cylinder-pickup). The suggestion that the basal ganglia is involved in the details of movement sequencing can,

however, be reconciled with the view of the basal ganglia as an action selection device on the grounds that such tasks can be regarded as action selection problems on a much shorter time-scale. Again, this is consistent with the evidence of multiple basal ganglia domains and the general hypothesis (Redgrave et al., 1999) that similar switching circuitry is employed in different regions of the basal ganglia to resolve selection problems at different levels of functional integration. It seems likely, however, that in the case of innate or well-practiced movement patterns, fine-grained control of movement, generally, takes place outside the basal ganglia. The research on the syntax of rat grooming behavior, reviewed above, serves to demonstrate this point—Cromwell and Berridge (1996) propose both that the role of sequencing the component movements of basic grooming acts is satisfied by pattern-generators in the brainstem, and that the role of the basal ganglia, "is not so much for the generation of the serial order pattern ⟨…⟩ as for the implementation of that pattern in the normal flow of behavior." (p. 3455). Research on learning in the striatum suggests a further interesting possibility in relation to acquired behaviour. Carelli, Wolske, & West (1997) have shown that striatal neurons that fire while a rat is learning a lever-pressing task cease firing once that behavior is well-practised. The conclusion these researchers derived from this finding is that the striatal activity needed to learn a particular motor response may not be required for its performance once the action has become automated. This result is open to a number interpretations, however, one possibility is that action selection by the basal ganglia may be involved in constructing new movement sequences which, following practice, then become available for selection as larger 'chunks' of behavior (Graybiel, 1998).

5.3.2. Activity in Substantia Nigra pars reticulata neurons during behavior

A number of recent studies with behaving rats (Gulley, Kosobud, & Rebec, 2002; Gulley, Kuwajima, Mayhill, & Rebec, 1999; Meyer-Luehmann et al., 2002) have noted correlations between SNr activity and episodes of motor behavior. Given the prevailing view that the basal ganglia selectively gate the motor system through the removal of EP/SNr inhibition, a particularly interesting finding is that rat SNr cells showing an increase in behavior-related firing generally out-number those showing a decrease in firing rate. For instance, Gulley et al. (1999) compared electrophysiological recordings of SNr cells during movement with those of the same neurons during periods of quiet rest. Of the cells showing an overall correlation with movement, 79% showed increased firing compared to 21% decreased firing. In cells with increased firing, rates were up to 38% higher than during the base-line rest period. In a further study (Gulley et al., 2002), comparing SNr activity during a conditioned reinforcement task with a base-line period prior to exposure to the reward-related apparatus, 110 of 225 SNr cells (48%) showed an increased in activation of 200% or more, while only 17 cells (8%) showed a decrease of 25% or greater.

The above findings concur with the levels of activity found in our model of EP/SNr during different patterns of robot activity. Specifically, we found fluctuations in EP/SNr output correlating with changes in channel salience, and a substantial increase (34–82%) in the average output of losing channels during episodes of partial or full selection as compared to periods of no selection (inactivity). It seems reasonable to expect that in action selection competitions mediated by the rat basal ganglia losers will outnumber winners (just as in the robot where there is generally 1 winner and 4 losers). Our model is, therefore, consistent with the data of Gulley et al. (2002, 1999) showing that only a minority of cells reduce their activity during behavior (here interpreted as the 'winning channels'), whilst a majority show increased activity (the 'losing channels'). Our analysis of the mechanisms underlying these changes suggests that SNr neurons showing increased firing are responding to correlated increases in STN, which in turn are due to greater activity in cortical-STN afferents, and in particular, in pathways encoding thalamocortical feedback from winning channels. Such increases can be expected to be most evident during periods of activity relative to inactivity (as in Gulley et al., 1999), or where there is a sudden increase in the affordances for reward-related behavior (as in Gulley et al., 2002).

5.3.3. Behavioral disintegration in competitions between multiple high-salience competitors

When presented with a continuous sequence of high salience selection competitions the robot exhibited two identifiable patterns of behavioral disintegration. First, it displayed reduced efficiency of the winning sub-system combined with partial activity of losing sub-systems. This resulted in a slowed and distorted execution of the most active behavior. Second, a 'behavioral trap' developed consisting of repeated switching between two behaviors. The latter pattern arose through the full selection, but premature interruption, of a fixed action pattern (*cylinder-pickup*), and depended on two features of the embedded model: (i) that intrinsically generated salience signals are used to maintain ongoing selections, and (ii) that the timing and maintenance of such signals relies upon feedback signals from the selection mechanism (that are disrupted under circumstances of strong, evenly matched salience). Possible neural correlates for these mechanisms were considered above (Section. 5.2).

Whilst the performance of the model in these circumstances is clearly sub-optimal from a purely action selection viewpoint, it shows interesting similarities to the findings of a large number of studies investigating the behavior of animals in conflict situations (Fentress, 1973; Hinde, 1953, 1966; Roeder, 1975). For instance, Hinde (1966) describes a number of possible outcomes that have been observed in ethological studies of strong behavioral

conflicts: (i) inhibition of all but one response, (ii) incomplete expression of a behavior (generally the preparatory stages of behavior are performed), (iii) alternation between behaviors (or 'dithering'), (iv) ambivalent behavior (a mixture of motor responses), (v) compromise behavior (similar to ambivalence, except that the pattern of motor activity is compatible with both behavioral tendencies), (vi) autonomic responses (for instance defecation or urination), (vii) displacement activity (expression of a behavior that seems irrelevant to the current motivational context, e.g. grooming in a 'fight or flight' conflict situation) . Of these outcomes, several show clear similarities with the behavior of the robot in the high salience condition. Specifically, the distortion observed in the early stages of the trial could be understood as a form of ambivalent behavior (iv), whilst the later repetitive behavioral switching has elements of both incomplete expression of behavior (ii) and alternation (iii).

More generally, the behavior of the embodied basal ganglia model is consistent a wide range of findings in psychology and ethology demonstrating that behavioral processes are most effective at intermediate levels of activation (Berlyne, 1960; Bindra, 1969; Fentress, 1973; Malmo, 1959), These findings can also be viewed as expressing the Yerkes-Dodson law (Yerkes & Dodson, 1908) that predicts an 'inverted U'-shaped relationship between arousal and performance. Our model is consistent with this law in that the robot shows little or no behavioral expression when only low salience inputs are present, demonstrates effective action selection for a range of intermediate level salience inputs (and for high salience inputs where there is no high salience competitor), and exhibits disintegrated behavior in circumstance of conflict between multiple high-salience systems. The robot model, therefore, suggests that the basal ganglia form an important element of the neural substrate mediating the effects of arousal on behavioral effectiveness.

5.4. Comparison with other modeling investigations of the basal ganglia

The literature on computational modeling of the basal ganglia has been extensively reviewed elsewhere (Gillies & Arbuthnott, 2000; Gurney et al., 2004; Houk Davis, & Beiser, 1995; Prescott et al., 2002). Whilst action selection is a strongly emerging theme in this literature, the Gurney et al. (2001a,b) model that we have embedded in our robot architecture is distinctive in its interpretation of basal ganglia intrinsic circuitry as containing synergistic 'selection' and 'control' pathways. The current study demonstrates the effectiveness of these mechanisms, when combined with basal ganglia thalamocortical loops, in providing effective robot action selection across a wide range of competing salience inputs. A large number of models have also examined the role of the basal ganglia as part of a wider circuit involved in motor control or behavioral sequencing (e.g. Bar-Gad, Morris, & Bergman, 2003; Beiser & Houk, 1998; Brown, Bullock, & Grossberg, 2004; Contrerasvidal & Stelmach, 1995; Dominey & Arbib, 1992; Dominey & Boussaoud, 1997; Frank, Loughry, & O'Reilly, 2001; Fukai, 1999; Houk & Wise, 1995; Taylor & Taylor, 2000) but have stopped short of investigating fully embodied (robotic) implementations. In the current article we have adopted a different strategy emphasizing embodiment as both a test-bed for validating hypotheses about basal ganglia function, and also as an 'intuition-pump' for generating new insights into neurobiological data. For instance, the requirement to provide integrated sequences of robot behavior that fulfill real goals, focused our attention on the problem of maintaining ongoing behavioral selections in the face of varying motivational and sensory input. Resolving these issues for the robot model then prompted us to reconsider evidence for striatal and thalamocortical activity during ongoing behavior as a possible neural substrate for this function of selection maintenance. Whilst some authors have assigned a role to basal ganglia thalamocortical loops in sustaining working memory patterns (e.g. Beiser & Houk, 1998; Frank et al., 2001), we suggest the more general hypothesis that these circuits operate to maintain ongoing selections in either the behavioral or working memory domains. Further, whereas Frank et al. (2001) have proposed a dissociation between intermittent firing in the basal ganglia that performs a gating role, and more continuous firing in frontal cortex that performs a maintenance role; we have drawn attention to the ongoing activity in basal ganglia during movement that cannot be linked to the initiation of new selections. We suggest that a parsimonious explanation of this activity, consistent with the wider hypothesis of selection by the basal ganglia, is that it serves to *maintain* selections and varies both with the urgency assigned to the completion of the current task (maintenance signals) and with the changing salience values of competitors (due to the dynamics of between-channel interactions in the basal ganglia).

The basal ganglia are strongly implicated in goal-directed or incentive learning (Dayan & Balleine, 2002; Hollerman, Tremblay, & Schultz, 2000; Kimura, 1995), a key finding in this context being that dopaminergic neurons in midbrain basal ganglia nuclei appear to fire in conjunction with rewarding events, or prior to anticipated rewarding events (Schultz, Apicella, & Ljungberg, 1993; Schultz et al., 1997). Montague and colleagues (Montague, Dayan, & Sejnowski, 1996; Schultz et al., 1997) have proposed that the afferents from these structures to striatal neurons may provide a training signal similar to the *temporal difference error* used in artificial reinforcement learning methods, while Houk, Adams, and Barto (1995) were the first of several authors to suggest that something akin to an *actor-critic* learning system (Sutton & Barto, 1998) may be operating in the basal ganglia. There have been various computational formulations of these proposals (see Doya, Dayan, & Hasselmo, 2002; Montague, Hyman,

& Cohen, 2004; Schultz, 1997; Worgotter & Porr, 2005 for reviews), including a robotic demonstration of a 'dopamine'-based actor-critic model described by (Sporns & Alexander, 2002). Despite this effort, there is no universally accepted theory, at a systems level, of how such learning might be implemented in the circuits of the basal ganglia (Joel, Niv, & Ruppin, 2002; Worgotter & Porr, 2005), and this remains a very active area of research. Our article has addressed the question of whether an embodied model of the basal ganglia can perform appropriate action selection irrespective of how the salience-related parameters for specific actions are determined; although hand-tuned parameters where used, the model could, in principle, be extended so as to learn from experience using model learning systems such as those reviewed above.

There is a general trend in basal ganglia modeling towards the use of more biologically realistic but computationally intensive models of neural circuits based on 'leaky-integrate and fire' (LIF) or compartmental models of single neurons (Gurney et al., 2004). The availability of parallel computing clusters is beginning to make feasible the simulation of large-scale circuits that include these more detailed single neuron models, at speeds that will permit real-time control of robot behavior. Future versions of our robot model will, therefore, seek to incorporate greater biological detail, for instance, by using a spike-coding (rather than rate-coding) neurons as our basic model element (Humphries, 2002), by incorporating additional pathways (Gurney et al., 2004), and by exploiting insights from biophysical modeling of single neurons (e.g. Wood et al., 2004). One particularly promising route may be to use so-called 'reduced' models (e.g. (Izhikevich, 2003; Rinzel & Ermentrout, 1998) that can exhibit many of the patterns of excitability shown in real neurons without the full apparatus of the Hodgkin–Huxley dynamics instantiated across several ionic currents (as required in biophysical models). An additional goal will be to incorporate realistic models of target sensor input and motor output systems—for instance, through embodied modeling of the role of the basal ganglia in sensorimotor tasks such as gaze control—in order to more directly address a wide range of neurobehavioral data.

6. Conclusion

We have described the robotic embedding of a high-level model of the basal ganglia and related nuclei based on the premise that these neural circuits play a critical role in action selection. This model was challenged with the task of selecting between five alternative behavioral sub-systems in the context of varying motivational and sensory inputs, and required to generate coherent sequences of robot behavior. Results demonstrate that the model basal ganglia switches effectively between competing sub-systems depending on the dynamics of their relative salience. The architecture, therefore, provides an existence proof that the basal ganglia can function as an effective action selection mechanism when embedded in a physical device. Further, by generating a model whose behavior is directly observable (rather than merely interpretable as a disembodied model would be) we were able to draw some interesting comparisons with the outcomes of behavioral experiments with animals, most notably with respect to: (i) the role of the basal ganglia in behavioral sequencing, (ii) the activity of neurons in basal ganglia input (striatum and STN) and output (SNr) nuclei during ongoing behavior, and (iii) the behavior of animals in situations of behavioral conflict.

Acknowledgements

The authors wish to acknowledge the assistance of Jonathan Chambers, Ric Wood, Michael Port, Andy Ham, and Olivier Michel, and the support of the UK Engineering and Physical Sciences Research Council (EPSRC) grant number GR/R95722.

Appendix A. Sensory systems

The first six peripheral sensors (1–6) are arranged in a semi-circle at the front of the robot, sensor 1 is furthest left, sensor 6 furthest right, with sensors 3 and 4 covering a narrow field of view directly ahead of the robot. Sensors 7 and 8 are directed towards the rear of the robot and are not used in the current model. The ith peripheral sensor generates both an infra-red proximity reading, ir(i), which is integer valued in the range 0–1023 with higher values indicating greater proximity to a nearby surface, and an ambient-light reading, amb(i), in the range 0–450 with lower values indicate greater luminance. The optical gripper sensor, opt( ), provides a binary signal, 1 if there is an object in the gripper, 0 otherwise. The arm position sensor, arm( ), returns a value in the range 255 (lowered in front) to 152 (raised overhead). The following variables are computed from the current infra-red and ambient light readings for use in determining motor vector values and perceptual and motivational variables:

$$ir_{\text{tot}} = \sum_{i=1}^{6} ir(i), \qquad ir_{\text{left}} = \sum_{i=1}^{3} ir(i), \qquad ir_{\text{right}} = \sum_{i=4}^{6} ir(i),$$

$$ir_{\text{diff}} = |ir_{\text{left}} - ir_{\text{right}}|, \qquad \text{side} = \begin{cases} \text{left}, & ir_{\text{left}} \geq ir_{\text{right}} \\ \text{right}, & \text{otherwise} \end{cases},$$

$$\text{detect}(i) = \begin{cases} 1, & ir(i) > 30 \\ 0, & \text{otherwise} \end{cases}, \qquad n_{\text{touch}} = \sum_{i=1}^{6} \text{detect}(i),$$

$$\text{lit}(i) = \begin{cases} 1, & \text{amb}(i) < 100 \\ 0, & \text{otherwise} \end{cases}, \qquad n_{\text{lit}} = \sum_{i=1}^{6} \text{lit}(i).$$

Table B1
The condition-action mapping employed by each action sub-system to generate a motor vector and a busy signal value (where needed) at each time-step

Cylinder-seek:		
$ir_{tot} \leq 500$	$v_{seek} = (0,1.00, 0,1.00, 0,0,0, 0,0)$	//no nearby objects //fast ahead
$ir_{tot} > 500$ and $n_{lit} \geqq 2$		//strong light (nest)
sd = left:	$v_{seek} = (0.27,0, 1.00,0, 0,0,0, 0,0)$	//backup, rotating right
sd = right:	$v_{seek} = (1.00,0, 0.27,0, 0,0,0, 0,0)$	//backup, rotating left
$500 < ir_{tot} \leq 1025$ and $n_{lit} < 2$	$v_{seek} = (0,1.00, 0,1.00, 0,0,0, 0,0)$	//nearby object //fast ahead
$1025 < ir_{tot} \leq 2000$ and $n_{lit} < 2$		//possible cylinder
side = left:	$v_{seek} = (0.20,0, 0,0.15, 0,0,0, 0,0)$	//rotate toward object
side = right:	$v_{seek} = (0,0.15, 0.20,0, 0,0,0, 0,0)$	//rotate toward object
	$ir_{tot} > 2000$ and $n_{lit} < 2$	//probable wall
side = left:	$v_{seek} = (0,nws, nws,0, 0,0,0, 0,0)$	//rotate away (right)
side = right:	$v_{seek} = (nws,0, 0,nws, 0,0,0, 0,0)$	//rotate away (left)
Wall-seek:		
$ir_{tot} \leq 10$	$v_{wall} = (0,1.0, 0,1.0, 0,0,0, 0,0)$	//in 'free space' //fast ahead
$10 < ir_{tot} \leq 500$	$v_{wall} = (0,0.50, 0,0.50, 0,0,0, 0,0)$	//some contact //slow ahead
$ir_{tot} > 500$		//near an obstacle
side = left:	$v_{wall} = (0,nws, nws,0, 0,0,0, 0,0)$	//rotate right
side = right:	$v_{wall} = (nws,0, 0,nws, 0,0,0, 0,0)$	//rotate left
wall-follow:		
$ir_{tot} \leq 600$		//well away from wall
side = left:	$v_{foll} = (0,0.20, 0,0.27, 0,0,0, 0,0)$	//veer-in sharp left
side = right:	$v_{foll} = (0,0.27, 0,0.20, 0,0,0, 0,0)$	//veer-in sharp right
if $600 < ir_{tot} < 1200$		//away from wall
side = left:	$v_{foll} = (0,sws, 0,fws, 0,0,0, 0,0)$	//veer-in left
side = right:	$v_{foll} = (0,fws, 0,sws, 0,0,0, 0,0)$	//veer-in right
$1200 \leq ir_{tot} < 2000$		//quite near wall
side = left:	$v_{foll} = (0,fws, 0,sws, 0,0,0, 0,0)$	//veer-out gently right
side = right:	$v_{foll} = (0,sws, 0,fws, 0,0,0, 0,0)$	//veer-out gently left
$ir_{tot} > 2000$		//very close to wall
side = left:	$v_{foll} = (0,0.15, 0.15,0, 0,0,0, 0,0)$	//rotate right
side = right:	$v_{foll} = (0.15,0, 0,0.15, 0,0,0, 0,0)$	//rotate left
$n_{touch} \neq 1$	$b_{foll} = 0$	
$n_{touch} = 1$	$b_{foll} = 1$	
Cylinder-pickup:		
$0 < t_{pick} < 0.3$	$b_{pick} = 0$, $v_{pick} = (0,0.10, 0,0.10, 0,0,0, 0,0)$	//slow approach
$0.3 \leq t_{pick} < 1.4$	$b_{pick} = 1$, $v_{pick} = (0.20,0, 0.20,0, 0,0,0, 1.0,0)$	//backup, open gripper
$1.4 \leq t_{pick} < 1.8$	$b_{pick} = 1$, $v_{pick} = (0,0, 0,0, 0,0,1.0, 0,0)$	//lower arm (floor)
$1.8 \leq t_{pick} < 2.8$	$b_{pick} = 1$, $v_{pick} = (0,0, 0,0, 0,0,0, 0,1.0)$	//close gripper
$2.8 \leq t < 3.5$	$b_{pick} = 1$, $v_{pick} = (0,0, 0,0, 1.0,0,0, 0,0)$	//raise arm (vertical)
$3.6 \leq t_{pick}$	$b_{pick} = 0$, $v_{pick} = (0,0, 0,0, 0,0,0, 0,0)$, $t = 0.0$	//idle
Cylinder-deposit:		
$0 < t_{dep} < 0.8$	$b_{dep} = 1$, $v_{dep} = (0,0, 0,0, 0,1.0,0, 0,0)$	//lower arm (horizontal)
$0.8 \leq t_{dep} < 1.6$	$b_{dep} = 1$, $v_{dep} = (0,0, 0,0, 0,0,0, 1.0,0)$	//release cylinder
$1.6 \leq t_{dep} < 2.4$	$b_{dep} = 1$, $v_{dep} = (0,0, 0,0, 1.0,0,0, 0,0)$	//raise arm (vertical)
$2.4 \leq t_{dep}$	$b_{dep} = 0$, $v_{dep} = (0,0, 0,0, 0,0,0, 0,0)$, $t = 0.0$	//idle

Appendix B. Action sub-systems

Each action sub-system generates a motor vector:

$$\mathbf{v} = [v_{lws-}, v_{lws+}, v_{rws-}, v_{rws+}, v_{vert}, v_{horiz}, v_{floor}, v_{open}, v_{close}]$$

where $0 \leq v_j \leq 1 \; \forall \; v_j \in \mathbf{v}$.

The first four elements of v correspond to the backward and forward components of the desired left (v_{lws-},v_{lws+}) and right (v_{rws-},v_{rws+}) wheel speeds, the next three to alternate positions for the arm (v_{vert},v_{horiz},v_{floor}) and the last two to instructions to open or close the gripper (v_{open}, v_{close}).

The following variable wheel speed values are computed based on current sensory input, for use by action

sub-systems:

$$\text{nws} = \begin{cases} 0.07, & ir_{\text{diff}} < 30 \\ ir_{\text{diff}}/450, & ir_{\text{diff}} < 450 \\ 1.0, & \text{otherwise} \end{cases},$$

$$\text{sws} = 0.4 - 5.0 \times 10^{-4} |ir_{\text{tot}} - 1200|,$$

$$\text{fws} = 0.4 - 3.5 \times 10^{-4} |ir_{\text{tot}} - 1200|.$$

The condition-action mapping employed by each action sub-system to generate a motor vector and a busy signal value (where needed), at each time-step, are given in Table B1 in pseudo code. Note that for the two 'fixed action patterns'—*cylinder-pickup* and *cylinder-deposit*—the condition element of the mapping indicates dependency on elapsed time (in seconds) since the start of the behavior as recorded by the relevant sub-system clock (t_{pick} or t_{dep}), see Section 3.3.2 for details.

Appendix C. Perceptual and motivational sub-systems

Detecting a wall. A wall is detected if the sum of infrared readings across all forward-facing sensors indicates a nearby surface *and either* the left-most(1) or right-most(6) sensor input suggest a nearby surface on that side or three or more of the forward sensors detect a surface at any distance (input > 30). These conditions are required to allow a wall to be detected when it is approached at any angle, or when the robot is moving parallel to a wall. A wall can only be detected when the arm is raised above horizontal (arm( ) < = 227) since, otherwise, the gripper arm will be detected as a wall (note that the gripper arm may still be responded to as a 'surface' by action sub-systems).

$$p_{\text{wall}} = \begin{cases} +1, & (ir_{\text{tot}} > 800) \\ & \wedge \left(\begin{array}{l} ir(1) > 800 \vee ir(6) > 800 \\ \vee \sum_{i=1}^{6} \text{detect}(i) \geq 3 \end{array} \right) \\ & \wedge (\text{arm}( ) < = 227) \\ -1, & \text{otherwise} \end{cases}$$

Detecting a nest: A nest is detected if the ambient light reading on at least two of the forward peripheral sensors is below a threshold, hence:

$$p_{\text{nest}} = \begin{cases} +1, & n_{\text{lit}} \geq 2 \\ -1, & \text{otherwise} \end{cases}$$

Detecting a cylinder. A cylinder is detected when the two front-most sensors (3 and 4) detect a surface at very close proximity, and the two sensors either side (2 and 5) of the front detect no surface. A cylinder cannot be detected in the nest (to prevent perceptual aliasing):

$$p_{\text{cyl}} = \begin{cases} +1, & (ir(2) < 10 \wedge ir(3) > 1000 \wedge ir(4) \\ & > 1000 \wedge ir(5) < 10) \wedge (p_{\text{nest}} \neq +1) \\ -1, & \text{otherwise} \end{cases}.$$

Gripper status. The gripper is considered to contain a cylinder when the optical sensor is triggered:

$$p_{\text{grip}} = \begin{cases} +1, & \text{grip}( ) = 1 \\ -1, & \text{otherwise} \end{cases}.$$

The simulated motivation m_{fear} is initialized to 1.0 and decays toward a minimum value of 0.0 at a rate of −0.0007 per step; the motivation m_{hung} is initialized to 0.2 and increases at a constant rate of +0.0015 per step toward a maximum of 1.0, except on any time-step where a cylinder is deposited in a 'nest' area at which point it falls immediately to 0.0.

Appendix D. The motor plant

The two wheel motors can be powered forwards and backwards and are controlled by integer-valued motor commands ranging from −20 (maximum reverse) to +20 (maximum advance). The robot gripper turret is powered by two motors, one to lift/lower the arm, the other to open/close the gripper. For the current model the useful range of operation for the arm motor varies from touching the floor (255), to overhead/vertical (152). The gripper motor is controlled by a binary command signal of 1 to close, 0 to open. To operate within these constraints the elements of the aggregate motor vector

$$\hat{\mathbf{v}} = [\hat{v}_{lws+}, \hat{v}_{lws-}, \hat{v}_{rws+}, \hat{v}_{rws-}, \hat{v}_{\text{up}}, \hat{v}_{\text{middle}}, \hat{v}_{\text{down}}, \hat{v}_{\text{open}}, \hat{v}_{\text{closed}}]$$

are converted into instructions to the four robot motors as follows

$$\text{wheels} : lws = 15(\hat{v}_{lws+} - \hat{v}_{lws-}),\ rws = 15(\hat{v}_{rws+} - \hat{v}_{rws-})$$

$$\text{arm} : \text{unless } \hat{v}_{\text{vert}} + \hat{v}_{\text{horiz}} + \hat{v}_{\text{floor}} = 0.0$$

$$\text{arm\_position} = \frac{152 \times \hat{v}_{\text{vert}} + 227 \times \hat{v}_{\text{horiz}} + 255 \times \hat{v}_{\text{floor}}}{\hat{v}_{\text{vert}} + \hat{v}_{\text{horiz}} + \hat{v}_{\text{floor}}}$$

$$\text{gripper} : \text{unless } \hat{v}_{\text{open}} + \hat{v}_{\text{closed}} = 0.0$$

$$\text{gripper\_position} = \begin{cases} 1(\text{closed}), & \hat{v}_{\text{closed}} - \hat{v}_{\text{open}} > 0.0 \\ 0(\text{open}), & \text{otherwise} \end{cases},$$

where all fractional values are rounded to the nearest integer.

References

Akkal, D., Burbaud, P., Audin, J., & Bioulac, B. (1996). Responses of substantia nigra pars reticulata neurons to intrastriatal D1 and D2 dopaminergic agonist injections in the rat. *Neuroscience Letters*, *213*(1), 66–70.

Albin, R. L., Young, A. B., & Penney, J. B. (1989). The functional anatomy of basal ganglia disorders. *Trends in Neurosciences*, *12*(10), 366–375.

Aldridge, J. W., Anderson, R. J., & Murphy, J. T. (1980). The role of the basal ganglia in controlling a movement initiated by a visually presented cue. *Brain Research*, *192*(1), 3–16.

Aldridge, J. W., & Berridge, K. C. (1998). Coding of serial order by neostriatal neurons: a 'natural action' approach to movement sequence. *Journal of Neuroscience*, *18*(7), 2777–2787.

Alexander, G. E., & Crutcher, M. D. (1990). Functional architecture of basal ganglia circuits: neural substrates of parallel processing. *Trends in Neurosciences*, *13*(7), 266–271.

Bar-Gad, J., Morris, G., & Bergman, H. (2003). Information processing, dimensionality reduction and reinforcement learning in the basal ganglia. *Progress in Neurobiology*, *71*, 439–473.

Barlow, G. W. (1977). Modal action patterns. In T. A. Sebeok (Ed.), *How Animals Communicate* (pp. 98–134). Bloomington, Indiana: Indiana University Press.

Basso, M. A., & Wurtz, R. H. (2002). Neuronal activity in substantia nigra pars reticulata during target selection. *Journal of Neuroscience*, *22*(5), 1883–1894.

Beiser, D. G., & Houk, J. C. (1998). Model of cortical-basal ganglionic processing: Encoding the serial order of sensory events. *Journal of Neurophysiology*, *79*(6), 3168–3188.

Berlyne, D. E. (1960). *Conflict, Arousal, and Curiosity*. New York: McGraw-Hill.

Bindra, D. (1969). An interpretation of the displacement phenomenon. *British Journal of Psychology*, *50*, 263–268.

Blomfield, S. (1974). Arithmetical operations performed by nerve cells. *Brain Research*, *69*(1), 115–124.

Brown, J. W., Bullock, D., & Grossberg, S. (2004). How laminar frontal cortex and basal ganglia circuits interact to control planned and reactive saccades. *Neural Networks*, *17*, 471–510.

Bryson, J. (2000). Cross-paradigm analysis of autonomous agent architecture. *Journal of Experimental and Theoretical Artificial Intelligence*, *12*(2), 165–189.

Buhusi, C. V., & Meck, W. H. (2002). Differential effects of methamphetamine and haloperidol on the control of an internal clock. *Behavioral Neuroscience*, *116*(2), 291–297.

Carelli, R. M., Wolske, M., & West, M. O. (1997). Loss of lever press-related firing of rat striatal forelimb neurons after repeated sessions in a lever pressing task. *Journal Of Neuroscience*, *17*(5), 1804–1814.

Casseday, J. H., & Covey, E. (1996). A neuroethological theory of the operation of the inferior colliculus. *Brain, Behavior, and Evolution*, *47*(6), 311–336.

Chevalier, G., & Deniau, J. M. (1984). Spatio-temporal organization of a branched tecto-spinal/tecto-diencephalic neuronal system. *Neuroscience*, *12*(2), 427–439.

Colgan, P. (1989). *Animal Motivation*. London: Chapman and Hall.

Contrerasvidal, J. L., & Stelmach, G. E. (1995). A neural model of basal ganglia-thalamocortical relations in normal and Parkinsonian movement. *Biological Cybernetics*, *73*(5), 467–476.

Cools, A. R. (1980). Role of the neostriatal dopaminergic activity in sequencing and selecting behavioural strategies: facilitation of processes involved in selecting the best strategy in a stressful situation. *Behavioural Brain Research*, *1*, 361–378.

Cowan, R. L., & Wilson, C. J. (1994). Spontaneous firing patterns and axonal projections of single corticostriatal neurons in the rat medial agranular cortex. *Journal of Neurophysiology*, *71*(1), 17–32.

Cromwell, H. C., & Berridge, K. C. (1996). Implementation of action sequences by a neostriatal site - a lesion mapping study of grooming syntax. *Journal Of Neuroscience*, *16*(10), 3444–3458.

Dayan, P., & Balleine, B. W. (2002). Reward, motivation, and reinforcement learning. *Neuron*, *36*(2), 285–298.

DeLong, M. R., Alexander, G. E., Georgopoulos, A. P., Crutcher, M. D., Mitchell, S. J., & Richardson, R. T. (1984). Role of basal ganglia in limb movements. *Human Neurobiology*, *2*(4), 235–244.

Denny-Brown, D., & Yanagisawa, N. (1976). The role of the basal ganglia in the initiation of movement. In M. D. Yahr (Ed.), *The basal ganglia* (pp. 115–149). New York: Raven Press.

Dominey, P. F., & Arbib, M. A. (1992). A cortico-subcortical model for generation of spatially accurate sequential saccades. *Cerebral Cortex*, *2*, 153–175.

Dominey, P. F., & Boussaoud, D. (1997). Encoding behavioral context in recurrent networks of the fronto-striatal system: a simulation study. *Cognitive Brain Research*, *6*, 53–65.

Doya, K., Dayan, P., & Hasselmo, M. E. (2002). Special Issue: Computational Models of Neuromodulation. *Neural Networks*, *15*, 475–774.

Elsinger, C. L., Rao, S. M., Zimbelman, J. L., Reynolds, N. C., Blindauer, K. A., & Hoffmann, R. G. (2003). Neural basis for impaired time reproduction in Parkinson's disease: an fMRI study. *Journal of the International Neuropsychological Society*, *9*(7), 1088–1098.

Ewert, J.-P. (1987). Neuroethology of releasing mechanisms: Prey-catching in toads. *Behavioral and Brain Sciences*, *10*, 337–389.

Ewert, J. P., Buxbaum-Conradi, H., Dreisvogt, F., Glagow, M., Merkel-Harff, C., Rottgen, A., et al. (2001). Neural modulation of visuomotor functions underlying prey-catching behaviour in anurans: perception, attention, motor performance, learning. *Comparative Biochemistry and Physiology A-Molecular & Integrative Physiology*, *128*(3), 417–461.

Fentress, J. C. (1973). Specific and nonspecific factors in the causation of behavior. In P. P. G. Bateson, & P. H. Klopfer (Eds.), *Perspectives in Ethology*. New York: Plenum Press.

Frank, M. J., Loughry, B., & O'Reilly, R. C. (2001). Interactions between frontal cortex and basal ganglia in working memory: a computational model. *Cognitive, Affective, and Behavioral Neuroscience*, *1*(2), 137–160.

Fukai, T. (1999). Sequence generation in arbitrary temporal patterns from theta- nested gamma oscillations: a model of the basal ganglia- thalamo-cortical loops. *Neural Networks*, *12*(7-8), 975–987.

Ganssle, J., & Barr, M. (2003). *Embedded Systems Dictionary*. Lawrence, KS: CMP Books.

Gerfen, C. R., Engber, T. M., Mahan, L. C., Susel, Z., Chase, T. N., Monsma, F. J., et al. (1990). D1 and D2 dopamine receptor regulated gene-expression of striatonigral and striatopallidal neurons. *Science*, *250*(4986), 1429–1432.

Gerfen, C. R., & Wilson, C. J. (1996). The basal ganglia. In L. W. Swanson, A. Bjorklund, & T. Hokfelt (Eds.), *Handbook of Chemical Neuroanatomy, Vol 12: Integrated Systems of the CNS, Part III* (pp. 371–468). Amsterdam: Elsevier.

Gibbon, J., Church, R. M., & Meck, W. H. (1984). Scalar timing in memory. *Annals of the New York Academy of Sciences*, *423*, 52–77.

Gillies, A., & Arbuthnott, G. (2000). Computational models of the basal ganglia. *Movement Disorders*, *15*(5), 762–770.

Girard, B., Cuzin, V., Guillot, A., Gurney, K. N., & Prescott, T. J. (2003). A basal ganglia inspired model of action selection evaluated in a robotic survival task. *Journal of Integrative Neuroscience*, *2*(2), 179–200.

Grace, A. A. (1991). Phasic versus tonic dopamine release and the modulation of dopamine system responsivity - a hypothesis for the etiology of schizophrenia. *Neuroscience*, *41*(1), 1–24.

Graybiel, A. M. (1998). The basal ganglia and chunking of action repertoires. *Neurobiology of Learning and Memory*, *70*, 119–136.

Gulley, J. M., Kosobud, A. E., & Rebec, G. V. (2002). Behavior-related modulation of substantia nigra pars reticulata neurons in rats performing a conditioned reinforcement task. *Neuroscience*, *111*(2), 337–349.

Gulley, J. M., Kuwajima, M., Mayhill, E., & Rebec, G. V. (1999). Behavior-related changes in the activity of substantia nigra pars reticulata neurons in freely moving rats. *Brain Research*, *845*(1), 68–76.

Gurney, K., Prescott, T. J., & Redgrave, P. (2001). A computational model of action selection in the basal ganglia I. A new functional anatomy. *Biological Cybernetics*, *84*(6), 401–410.

Gurney, K., Prescott, T. J., & Redgrave, P. (2001). A computational model of action selection in the basal ganglia II. Analysis and simulation of behaviour. *Biological Cybernetics*, *84*(6), 411–423.

Gurney, K., Prescott, T. J., Wickens, J., & Redgrave, P. (2004). Computational models of the basal ganglia: from membranes to robots. *Trends in Neurosciences*, *27*, 453–459.

Gurney, K. N., Humphries, M., Wood, R., Prescott, T. J., & Redgrave, P. (2004). Testing computational hypotheses of brain systems function: a case study with the basal ganglia. *Network*, *15*(4), 263–290.

Handel, A., & Glimcher, P. W. (1999). Quantitative analysis of substantia nigra pars reticulata activity during a visually guided saccade task. *Journal of Neurophysiology*, *82*(6), 3458–3475.

Harsing, L. G., & Zigmond, M. J. (1997). Influence of dopamine on GABA release in striatum: Evidence for D-1-D-2 interactions and non-synaptic influences. *Neuroscience*, *77*(2), 419–429.

Hikosaka, O. (1994). Role of basal ganglia in control of innate movements, learned behavior and cognition—a hypothesis. In G. Percheron, J. S. McKenzie, & J. Feger (Eds.), *The Basal Ganglia IV*. New York: Plenum.

Hikosaka, O., & Wurtz, R. H. (1989). The basal ganglia. In E. H. Wurtz, & M. E. Goldberg (Eds.), *The Neurobiology of Saccadic Eye Movements* (pp. 257–281). Amsterdam: Elsevier.

Hinde, R. A. (1953). The conflict between drives in the courtship and copulation of the Chaffinch. *Behaviour*, *5*, 1–31.

Hinde, R. A. (1966). *Animal Behaviour: a Synthesis of Ethology and Comparative Psychology*. London: McGraw-Hill.

Hollerman, J. R., Tremblay, L., & Schultz, W. (2000). Involvement of basal ganglia and orbitofrontal cortex in goal-directed behavior. *Progress in Brain Research*, *126*, 193–215.

Houk, J. C., Adams, J. L., & Barto, A. G. (1995). A model of how the basal ganglia generate and use neural signals that predict reinforcement. In J. C. Houk, J. L. Davis, & D. G. Beiser (Eds.), *Models of Information Processing in the Basal Ganglia*. Cambridge, MA: MIT Press.

Houk, J. C., Davis, J. L., & Beiser, D. G. (1995). *Models of Information Processing in the Basal Ganglia*. Cambridge, MA: MIT Press.

Houk, J. C., & Wise, S. P. (1995). Distributed modular architectures linking basal ganglia, cerebellum, and cerebral-cortex - their role in planning and controlling action. *Cerebral Cortex*, *5*(2), 95–110.

Houston, A., & Sumida, B. (1985). A positive feedback model for switching between 2 activities. *Animal Behaviour*, *33*(FEB), 315–325.

Hoyle, G. (1984). The scope of neuroethology. *The Behavioural and Brain Sciences*, *7*(3), 367–412.

Humphries, M. D. (2002). *The Basal Ganglia and Action: A Computational Study at Multiple Levels of Abstraction*. Unpublished PhD, University of Sheffield, Sheffield.

Humphries, M. D., & Gurney, K. N. (2001). A pulsed neural network model of bursting in the basal ganglia. *Neural Networks*, *14*, 845–863.

Humphries, M. D., & Gurney, K. N. (2002). The role of intra-thalamic and thalamocortical circuits in action selection. *Network: Computation in Neural Systems*, *13*, 131–156.

Humphries, M. D., Prescott, T. J., & Gurney, K. N. (2003). The interaction of recurrent axon collateral networks in the basal ganglia. In E. A. O. Kaynak, E. Oja, & L. Xu (Eds.), *Artificial Neural Networks and Neural Information Processing - ICANN/ICONIP 2003 (Lecture Notes in Computer Science 2714)* (pp. 797–804). Berlin: Springer.

Izhikevich, E. M. (2003). Simple model of spiking neurons. *IEEE Transactions on Neural Networks*, *14*(6), 1569–1572.

Jaeger, D., Gilman, S., & Aldridge, J. W. (1995). Neuronal activity in the striatum and pallidum of primates related to the execution of externally cued reaching movements. *Brain Research*, *694*, 111–127.

Joel, D., Niv, Y., & Ruppin, E. (2002). Actor-critic models of the basal ganglia: new anatomical and computational perspectives. *Neural Networks*, *15*(4-6), 535–547.

Joel, D., & Weiner, I. (1994). The organization of the basal ganglia-thalamocortical circuits - open interconnected rather than closed segregated. *Neuroscience*, *63*(2), 363–379.

Joseph, J. P., Boussaoud, D., & Biguer, B. (1985). Activity of neurons in the cat substantia nigra pars reticulata during drinking. *Experimental Brain Research*, *60*(2), 375–379.

Kermadi, I., & Boussaoud, D. (1995). Role of the primate striatum in attention and sensorimotor processes: comparison with premotor cortex. *Neuroreport*, *6*(8), 1177–1181.

Kermadi, I., & Joseph, J. P. (1995). Activity in the caudate nucleus of monkey during spatial sequencing. *Journal of Neurophysiology*, *74*(3), 911–933.

Kimura, M. (1995). Role of basal ganglia in behavioral learning. *Neuroscience Research*, *22*(4), 353–358.

Koch, C., Poggio, T., & Torre, V. (1983). Nonlinear interactions in a dendritic tree: localization, timing, and role in information processing. *Proceedings of the National Academy of Science USA*, *80*(9), 2799–2802.

Krout, K. E., Loewy, A. D., Westby, G. W., & Redgrave, P. (2001). Superior colliculus projections to midline and intralaminar thalamic nuclei of the rat. *Journal of Comparative Neurology*, *431*(2), 198–216.

Latimer, C. (1995). Computer modelling of cognitive processes. *Noetica: Open Forum*, *1*(1) (http://psy.uq.edu.au/CogPsych/Noetica/).

Lehner, P. N. (1996). *Handbook of Ethological Methods* (2nd ed). Cambridge, UK: Cambridge University Press.

Levesque, M., Charara, A., Gagnon, S., Parent, A., & Deschenes, M. (1996) . Corticostriatal projections from layer V cells in rat are collaterals of long-range corticofugal axons. *Brain Research*, *709*(2), 311–315.

Lorenz, K. (1935). Der kumpan in der umwelt des vogels. *Journal of Ornithology*, *83*, 137–213 (pp. 289–413).

Maes, P. (1995). Modelling adaptive autonomous agents. In C. G. Langton (Ed.), *Artificial Life: An Overview*. Cambridge, MA: MIT Press.

Malmo, R. (1959). Activation: a neuropsychological dimension. *Psychological Review*, *66*, 367–386.

Marin, O., Gonzalez, A., & Smeets, W. (1997). Anatomical substrate of amphibian basal ganglia involvement in visuomotor behaviour. *European Journal of Neuroscience*, *9*(10), 2100–2109.

Marsden, C. D., & Obeso, J. A. (1994). The function of the basal ganglia and the paradox of stereotaxic surgery in Parkinson's disease. *Brain*, *117*, 877–897.

Massaro, D. W. (1988). Some criticisms of connectionist models of human performance. *Journal of Memory and Language*, *27*, 213–234.

Matell, M. S., & Meck, W. H. (2000). Neuropsychological mechanisms of interval timing behavior. *Bioessays*, *22*(1), 94–103.

McFarland, D. (1989). *Problems of Animal Behaviour*. Harlow, UK: Longman.

McFarland, D., & Bosser, T. (1993). *Intelligent Behaviour in Animals and Robots*. Cambridge, MA: MIT Press.

Meck, W. H. (1983). Selective adjustment of the speed of internal clock and memory processes. *Journal of Experimental Psychology: Animal Behavior Processes*, *9*(2), 171–201.

Meck, W. H., & Benson, A. M. (2002). Dissecting the brain's internal clock: how frontal-striatal circuitry keeps time and shifts attention. *Brain and Cognition*, *48*(1), 195–211.

Meyer-Luehmann, M., Thompson, J. F., Berridge, K. C., & Aldridge, J. W. (2002). Substantia nigra pars reticulata neurons code initiation

of a serial pattern: implications for natural action sequences and sequential disorders. *European Journal of Neuroscience*, *16*(8), 1599–1608.

Mink, J. W. (1996). The basal ganglia: Focused selection and inhibition of competing motor programs. *Progress In Neurobiology*, *50*(4), 381–425.

Mink, J. W., & Thach, W. T. (1991). Basal ganglia motor control. II. Late pallidal timing relative to movement onset and inconsistent pallidal coding of movement parameters. *Journal of Neurophysiology*, *65*(2), 301–329.

Montague, P. R., Dayan, P., & Sejnowski, T. J. (1996). A framework for mesencephalic dopamine systems based on predictive hebbian learning. *Journal Of Neuroscience*, *16*(5), 1936–1947.

Montague, P. R., Hyman, S. E., & Cohen, J. D. (2004). Computational roles for dopamine in behavioural control. *Nature*, *431*(7010), 760–767.

Montes Gonzalez, F., Prescott, T. J., Gurney, K., Humphries, M., & Redgrave, P. (2000). An embodied model of action selection mechanisms in the vertebrate brain. In J. A. Meyer (Ed.), *From Animals to Animats 6: Proceedings of the 6th International Conference on the Simulation of Adaptive Behavior* (pp. 157–166). Cambridge, MA: MIT Press.

Mulder, A. B., Tabuchi, E., & Wiener, S. I. (2004). Neurons in hippocampal afferent zones of rat striatum parse routes into multi-pace segments during maze navigation. *European Journal of Neuroscience*, *19*(7), 1923–1932.

Parent, A., & Hazrati, L. N. (1995). Functional anatomy of the basal ganglia. II. The place of subthalamic nucleus and external pallidum in basal ganglia circuitry. *Brain Research Reviews*, *20*(1), 128–154.

Pinker, S., & Prince, A. (1988). On language and connectionism: analysis of a parallel distributed processing model of language acquisition. *Cognition*, *28*, 73–193.

Prescott, T. J., Gurney, K., & Redgrave, P. (2002). Basal ganglia. In M. A. Arbib (Ed.), *The Handbook of Brain Theory and Neural Networks*, 2nd ed (pp. 147–151). Cambridge, MA: MIT Press.

Prescott, T. J., Redgrave, P., & Gurney, K. N. (1999). Layered control architectures in robots and vertebrates. *Adaptive Behavior*, *7*(1), 99–127.

Redgrave, P., Prescott, T., & Gurney, K. N. (1999). The basal ganglia: a vertebrate solution to the selection problem? *Neuroscience*, *89*, 1009–1023.

Redgrave, P., Prescott, T. J., & Gurney, K. (1999). Is the short latency dopamine burst too short to signal reward error? *Trends in Neurosciences*, *22*, 146–150.

Reeves, G. (1998). *Re: What really happened on Mars*. Retrieved 54, 19, from http://catless.ncl.ac.uk/Risks/19.54.html.

Rinzel, J., & Ermentrout, E. (1998). Analysis of neural excitability and oscillations. In C. Koch, & I. Segev (Eds.), *Methods in Neuronal Modelling*. Cambridge, MA: MIT Press.

Robbins, T. W., & Brown, V. J. (1990). The role of the striatum in the mental chronometry of action: a theoretical review. *Reviews in the Neurosciences*, *2*, 181–213.

Roeder, K. D. (1975). Feedback, spontaneous activity, and behaviour. In G. Baerends, C. Beer, & A. Manning (Eds.), *Function and Evolution in Behaviour*. Oxford: Clarendon Press.

Ryan, L. J., & Clark, K. B. (1991). The role of the subthalamic nucleus in the response of globus- pallidus neurons to stimulation of the prelimbic and agranular frontal cortices in rats. *Experimental Brain Research*, *86*(3), 641–651.

Schmitzer-Torbert, N., & Redish, A. D. (2004). Neuronal activity in the rodent dorsal striatum in sequential navigation: separation of spatial and reward responses on the multiple T task. *Journal of Neurophysiology*, *91*(5), 2259–2272.

Schultz, W. (1986). Activity of pars reticulata neurons of monkey substantia nigra in relation to motor, sensory, and complex events. *Journal of Neurophysiology*, *55*(4), 660–677.

Schultz, W. (1997). Dopamine neurons and their role in reward mechanisms. *Current Opinion in Neurobiology*, *7*, 191–197.

Schultz, W., Apicella, P., & Ljungberg, T. (1993). Responses of monkey dopamine neurons to reward and conditioned stimuli during successive steps of learning a delayed response task. *Journal Of Neuroscience*, *13*(3), 900–913.

Schultz, W., Dayan, P., & Montague, P. R. (1997). A neural substrate for prediction and reward. *Science*, *275*, 1593–1599.

Sha, L., Rajkumar, R., & Lehoczky, J. P. (1990). Priority inheritance protocols: An approach to real-time synchronization. *IEEE Transactions on Computers*, *39*, 1175–1185.

Shibata, R., Mulder, A. B., Trullier, O., & Wiener, S. I. (2001). Position sensitivity in phasically discharging nucleus accumbens neurons of rats alternating between tasks requiring complementary types of spatial cues. *Neuroscience*, *108*(3), 391–411.

Shink, E., Sidibe, M., & Smith, Y. (1997). Efferent connections of the internal globus pallidus in the squirrel monkey: II. Topography and synaptic organization of pallidal efferents to the pedunculopontine nucleus. *Journal of Comparative Neurology*, *382*(3), 348–363.

Smith, Y., Bevan, M. D., Shink, E., & Bolam, J. P. (1998). Microcircuitry of the direct and indirect pathways of the basal ganglia. *Neuroscience*, *86*, 353–387.

Sporns, O., & Alexander, W. H. (2002). Neuromodulation and plasticity in an autonomous robot. *Neural Networks*, *15*(4-6), 761–774.

Sutton, R. S., & Barto, A. G. (1998). *Reinforcement learning: an introduction*. Cambridge, MA: MIT Press.

Taylor, J. G., & Taylor, N. R. (2000). Analysis of recurrent cortico-basal ganglia-thalamic loops for working memory. *Biological Cybernetics*, *82*(5), 415–432.

Tinbergen, N. (1951). *The Study of Instinct*. Oxford: Clarendon Press.

Toates, F. (1998). The interaction of cognitive and stimulus-response processes in the control of behaviour. *Neuroscience and Biobehavioral Reviews*, *22*(1), 59–83.

Tsumori, T., & Yasui, Y. (1997). Organization of the nigro-tecto-bulbar pathway to the parvicellular reticular formation: a light- and electron-microscopic study in the rat. *Experimental Brain Research*, *116*(2), 341–350.

Ulrich, D. (2003). Differential arithmetic of shunting inhibition for voltage and spike rate in neocortical pyramidal cells. *European Journal of Neuroscience*, *18*(8), 2159–2165.

Walters, J. R., Ruskin, D. N., Allers, K. A., & Bergstrom, D. A. (2000). Pre- and postsynaptic aspects of dopamine-mediated transmission. *Trends in Neurosciences*, *23*(10), S41–S47.

Wickens, J. (1997). Basal ganglia: structure and computations. *Network-Computation in Neural Systems*, *8*(4), R77–R109.

Wilson, C. J., & Kawaguchi, Y. (1996). The origins of two-state spontaneous membrane potential fluctuations of neostriatal spiny neurons. *Journal of Neuroscience*, *16*(7), 2397–2410.

Wood, R., Gurney, K. N., & Wilson, C. J. (2004). A novel parameter optimisation technique for compartmental models applied to a model of a striatal medium spiny neuron. *Neurocomputing*, *58-60*, 1109–1116.

Worgotter, F., & Porr, B. (2005). Temporal sequence learning, prediction, and control: a review of different models and their relation to biological mechanisms. *Neural Computation*, *17*(2), 245–319.

Yerkes, R. M., & Dodson, J. D. (1908). The relation of strength of stimulus to rapidity of habit formation. *Journal of Comparative Neurology and Psychology*, *18*, 459–482.

Zink, C. F., Pagnoni, G., Martin, M. E., Dhamala, M., & Berns, G. S. (2003). Human striatal response to salient nonrewarding stimuli. *Journal of Neuroscience*, *23*(22), 8092–8097.